University of Groningen

Sources of iron in the Ross Sea Polynya in early summer

Gerringa, L. J. A.; Laan, P.; van Dijken, G. L.; van Haren, H.; De Baar, H. J. W.; Arrigo, K. R.; Alderkamp, A. -C.

IMPORTANT NOTE: You are advised to consult the publisher's version (publisher's PDF) if you wish to cite from it. Please check the document version below.

Document Version
Publisher's PDF, also known as Version of record

Publication date:
2015

[Link to publication in University of Groningen/UMCG research database](#)
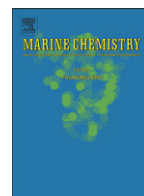
Sources of iron in the Ross Sea Polynya in early summer

L.J.A. Gerringa [a,*], P. Laan [a], G.L. van Dijken [b], H. van Haren [a], H.J.W. De Baar [a,c], K.R. Arrigo [b], A.-C. Alderkamp [b]

[a] Royal Netherlands Institute for Sea Research (NIOZ), PO Box 59, 1790 AB Den Burg, the Netherlands
[b] Department of Earth System Science, Stanford University, USA
[c] Department of Ocean Ecosystems, Energy and Sustainability Research Institute Groningen, University of Groningen, Groningen, The Netherlands

ARTICLE INFO

ABSTRACT

Dissolved Fe (DFe) was measured in the Ross Sea Polynya (RSP), Antarctica, during a GEOTRACES cruise between 20 December 2013 and 5 January 2014. DFe was measured over the full water column with special emphasis on samples near the seafloor. In the upper mixed layer, DFe was very low everywhere (<0.10 nM). DFe increased with depth to values between 0.60 and 2.76 nM near the seafloor. The highest DFE concentrations were found at stations where a bottom nepheloid layer (BNL) was present (28 out of 32 stations). Deep DFe was lower (0.24–0.38 nM) at stations with no BNL. The main DFe supply to the upper mixed layer was vertical diffusive transport from the seafloor sediments, with a mean flux of 3.3×10^{-8} mol DFe m^{-2} day^{-1}. DFe fluxes showed large spatial variability of three orders of magnitude and were positively correlated to DFe concentrations near the sediment and vertical turbulent eddy diffusivity (K_z) and negatively correlated to water depth. The greatest fluxes were observed above the shallow banks such as Ross and Pennell Banks, and sediments with a BNL. We studied the horizontal diffusive transport from Franklin Island as an example of horizontal DFe transport from landmasses. No DFe transport was detected in the upper 100 m of the water column, probably due to uptake by phytoplankton. However, at 200 and 300 m depth, the DFe transport at distances between 50 and 100 km from Franklin Island was as large as the mean diffusive upward transport, indicating the potential importance of landmasses as a local source of DFe. Conversely, no horizontal transport of DFe from banks was detected. In addition, the Ross Ice Shelf (RIS) was a negligible source of DFe. Only the Ice Shelf Water (ISW), a water mass formed under the RIS, contained slightly elevated DFe (0.18–0.26 nM) compared to the surrounding waters. However, this elevated DFe did not reach into the RSP. Icebergs were not encountered and were not evaluated as a DFe source. Overall, we conclude that DFe from the seafloor and land mass sediments are the main DFe sources of DFe that support phytoplankton in the upper mixed layer of the Ross Sea Polynya in early summer.

1. Introduction

Antarctic shelf waters are a strong sink for atmospheric CO_2 due to high biological productivity, intense winds, high air–sea gas exchange, formation of bottom water and extensive winter ice cover (Arrigo et al., 2008a; Jones et al., 2015-in this issue). These factors make these regions important for the biogeochemical cycling of elements, particularly that of carbon (Sarmiento et al., 2004; Arrigo et al., 2008a). Specifically, coastal polynyas (areas of open water surrounded by ice) are hot spots for energy and carbon transfer between the atmosphere and ocean (Smith and Barber, 2007). The reduced ice cover increases air–sea gas exchange and results in enhanced light availability in the near surface waters in early spring, thereby increasing primary productivity through phytoplankton photosynthesis. In addition to its importance for the global carbon cycle, phytoplankton productivity on Antarctic shelves supports the biota of higher trophic levels such as krill, penguins, and whales (Arrigo et al., 2003; Arrigo and Van Dijken, 2003a; Ainley et al., 2006).

In the Southern Ocean, phytoplankton productivity is often limited by the availability of iron (Fe) (de Baar et al., 1990; Martin et al., 1990, 1994; Boyd et al., 2007 and references therein), although light limitation due to deep vertical mixing may also limit phytoplankton growth (Mitchell et al., 1991; De Baar et al., 2005). Fe exists in both dissolved and particulate forms in seawater. Dissolved Fe (DFe) is considered to be the preferred form for phytoplankton, but since Fe has a low solubility in seawater, it easily precipitates or is scavenged, and sinks out of the euphotic zone as particulate Fe (Millero, 1998; Liu and Millero, 2002). The concentrations of DFe in Antarctic waters are controlled by a balance between Fe input from various sources, processes like organic complexation that keep Fe in solution, and removal processes (Gledhill and Van den Berg, 1994; Boyd et al., 2012; Klunder et al., 2011; Thuróczy et al., 2011, 2012). Dissolved organic ligands are molecules that bind trace metals such as Fe. In this way, the ligands increase the solubility of Fe, retard the precipitation of Fe (hydr-) oxides, and increase Fe availability for biological uptake in the upper ocean. As such, the binding by dissolved organic ligands may play an important role

* Corresponding author.

in the dissolution of Fe and keeping Fe in the dissolved phase. It is unknown which fraction of the organically complexed Fe pool can be directly utilized by phytoplankton and how it is taken up (Hassler et al., 2011; Gledhill and Buck, 2012).

Potential sources of DFe in Antarctic waters are upwelling of DFe-rich deep waters (De Baar et al., 1995; Löscher et al., 1997: Croot et al., 2004; Klunder et al., 2011), melting glaciers, ice sheets, and icebergs (De Baar et al., 1995; Raiswell et al., 2006, 2008; Gerringa et al., 2012; Wadham et al., 2013), melting sea ice (Sedwick and DiTullio, 1997; Lannuzel et al., 2010, 2014; van der Merwe et al., 2011), atmospheric dust deposition either directly into surface waters or onto sea ice (Croot et al., 2007; Sedwick et al., 2008, 2011; de Jong et al., 2013), hydrothermal vents (Tagliabue et al., 2010; Klunder et al., 2011; Hawkes et al., 2013; Aquilina et al., 2014), and sediment resuspension and reductive dissolution (Fitzwater et al., 2000; Sedwick et al., 2011; De Jong et al., 2012; Hatta et al., 2013; Marsay et al., 2014). Sediment resuspension and reductive dissolution are particularly important when a bottom nepheloid layer (BNL) is present, a layer above the sediment that contains significant amounts of suspended sediment, as it is important for exchange of DFe between sediment and water (Bacon and Rutgers van der Loeff, 1989; Klunder et al., 2012). Horizontal and vertical advection and diffusion determine the distribution of DFe from these sources (Blain et al., 2007, 2008; Gerringa et al., 2012; de Jong et al., 2012; Bowie et al., 2014), which is facilitated by complexation with dissolved organic ligands (Thuróczy et al., 2011, 2012; Boye et al., 2001; Croot et al., 2004; Gerringa et al., 2008).

The Ross Sea is one of the most studied coastal regions of Antarctica and the most productive sector of the Southern Ocean (Arrigo and Van Dijken, 2003a; Arrigo et al., 2008b). Low DFe concentrations have been reported in the surface waters, which may limit phytoplankton growth (Martin et al., 1990; Sedwick and DiTullio, 1997; Fitzwater et al., 2000; Coale et al., 2005; Sedwick et al., 2011; Marsay et al., 2014). Traditionally, it was thought that DFe concentrations in surface waters were high during the winter and early spring due to remineralization of Fe and vertical mixing that brings deep DFe-rich water to the surface (Sedwick and DiTullio, 1997; Fitzwater et al., 2000; Coale et al., 2005). This winter stock of DFe would then be taken up by phytoplankton over the course of the spring and summer, resulting in seasonal Fe-limitation of phytoplankton growth (Sedwick et al., 2000; Coale et al., 2005). However, Sedwick et al. (2011) showed that even in early spring, before the seasonal peak in phytoplankton abundance, DFe concentrations were already extremely low in surface waters of the Ross Sea Polynya (RSP). These low DFe concentrations were potentially limiting phytoplankton growth and suggest that bioavailable Fe must be supplied throughout the growing season in order to sustain phytoplankton blooms. However, the source of this DFe is unclear. The Ross Ice Shelf (RIS) does not appear to be a major source of DFe to surface waters of the RSP since DFe is relatively low at stations close to the edge of the RIS (Sedwick et al., 2011; Marsay et al., 2014). This contrasts with the Amundsen Sea, where the Pine Island Glacier was the main Fe source for the phytoplankton bloom in the Pine Island Polynya (Gerringa et al., 2012; Alderkamp et al., 2012), and the Dotson Ice Shelf was a major DFe source for phytoplankton in the Amundsen Sea Polynya (Sherrell et al., submitted; Alderkamp et al., 2015). Sedwick et al. (2011) suggested that the main Fe sources to surface waters of the Ross Sea were dust deposition, sea ice melt, and vertical exchange of DFe through reductive dissolution of sediments. Marsay et al. (2014) also suggested that sediment-derived Fe was the most important DFe source. De Jong et al. (2013) acknowledged the importance of dust and sea ice melt but also proposed that sediment-derived Fe from the melting of icebergs and ice sheets was an important DFe source. In contrast, Coale et al. (2005) concluded that DFe transport from the sediment through vertical mixing did not bring DFe to surface waters.

The research presented here aims to identify and quantify the sources of DFe that support phytoplankton blooms in the Ross Sea.

We present water column DFe concentrations related to water masses in the Ross Sea during December and January when the phytoplankton bloom typically reaches its highest biomass levels (Arrigo and Van Dijken, 2003a, 2004). In particular, we use high spatial resolution DFe concentration data from waters near suspected Fe sources, such as the Ross Ice Shelf, sea ice, sediments, Modified Circumpolar Deep Water (MCDW), and land masses (e.g., Franklin Island), to calculate DFe fluxes from these sources to surface waters where it supports phytoplankton growth.

2. Methods

2.1. Sampling

The cruise NBP13-10 of the RVIB *Nathaniel B. Palmer* took place from December 2013 to January 2014 as part of the Phantastic project. We entered the Ross Sea from the north-east on 20 December and left on the north-western side on 5 January (Fig. 1). We sampled a total of 33 stations, two stations in the eastern Ross Sea and 31 stations in the RSP (Fig. 1). Twenty-five stations made a circle section through the RSP that was sampled starting at station 20, going south to the RIS, and then counter-clockwise (Fig. 1).

The following sections will be discussed in detail:

1) The south–north central RSP transect along the 177.5°E meridian from a distance of 10 km from the RIS at 77.74°S to the north crossing one trough up to the Ross Bank and crossing a second trough to the Pennell Bank at 74.5°S. Along this section, we studied surface DFe in relation to water properties in the central RSP and potential DFe sources from the RIS and Ross Bank.
2) The east–west Pennell Bank transect along 74.5°S from the Pennell Bank at 177.5°E to the Joides Trough at 172.5°E. Here we studied potential DFe sources from the Pennell Bank.
3) The west–east Franklin Island transect along 76.1°S from 9.5 km east of Franklin Island at 168.7°E to 169°E. Along this section, we studied potential DFe sources from Franklin Island.
4) The western RSP transect, from station 75 (74.5°S, 172.5°E) moving to the south-west to station 87 (76°S, 170°E) and from there to the south-east (via st. 91, 101, 111, 112, 113) to station 114 (77.33°S, 177.5°E) which is the same position as station 31 of the central RSP transect. At this section, we studied surface DFe in relation to water properties in the western RSP.

All trace metal clean (TMC) water samples were collected using modified 12 L GO-FLO (Oceanics) samplers provided by the Royal NIOZ (The Netherlands) which were attached to a TMC frame provided by the United States Antarctic Program. Temperature, depth, and salinity were measured with a SBE 9/11*plus* conductivity–temperature–depth (CTD) system (SeaBird Electronics). The frame also included a C-star transmissometer (WET Labs) and a chlorophyll *a* (Chl *a*) fluorometer (WET Labs). Temperature and salinity were transformed into conservative temperature (Θ in °C) and absolute salinity (S$_A$ in g kg^{-1}) according to McDougall et al. (2009).

Typical sample depths were 10, 25, 50, 75, 100, and every 100 m, thereafter depending on water depth. Full water column profiles were sampled at 33 stations where the deepest sample was 6 ± 4.19 m above the bottom and an additional sample 10 m above the deepest sample. Occasionally, surface waters were sampled at 4–5 m depth.

Water was filtered (Sartorius®, 0.2 μm; Satrobran 300) prior to DFe analysis (see below) inside a trace metal clean van.

2.2. Analyses

2.2.1. DFe determination with Flow Injection Analysis

Trace metal clean work was done free from contamination in a plastic bubble on the ship. Overpressure in the bubble was achieved by
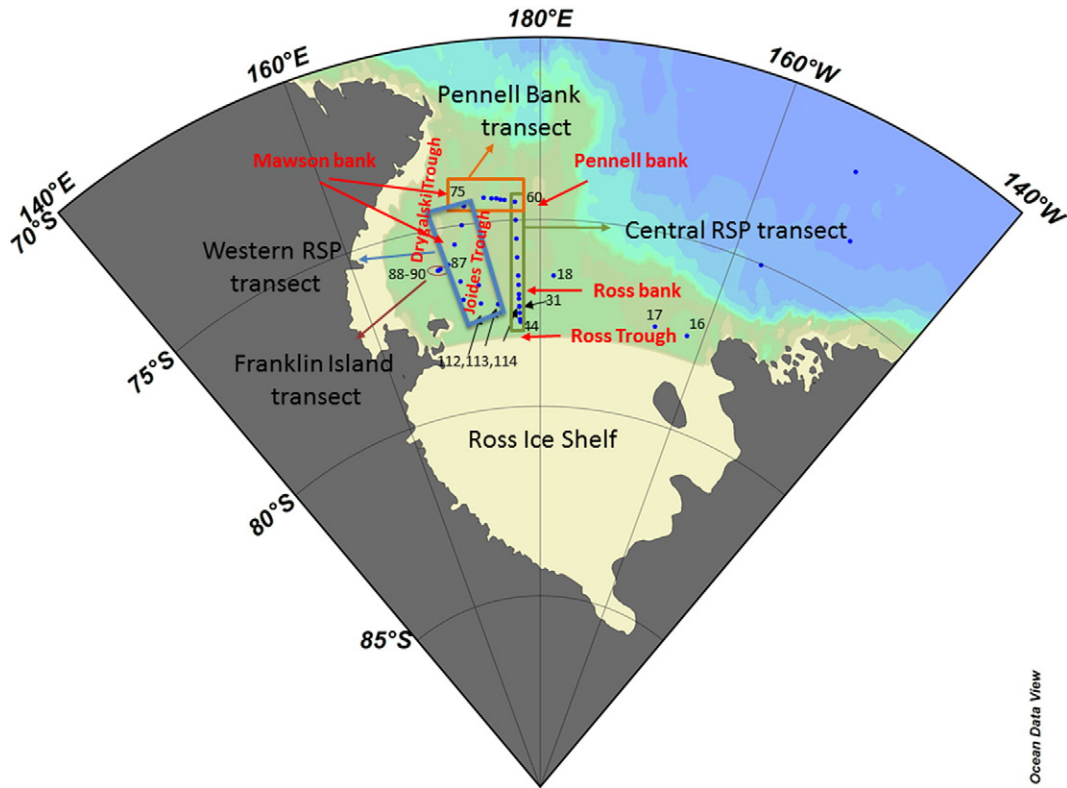
Fig. 1. Station map of the Ross Sea during the Phantastic cruise. Stations 16, 17, and 18 are east of the various transects. The circle transect consists of the central RSP, Pennell Bank and Western RSP transects. All station numbers are specified per transect in the method section 2.1. Station 114 has the same position as station 31.

inflow of air through a HEPA filter. Sample handling was done within a laminar flow bench inside the bubble.

DFe concentrations were measured directly on board by the automated Flow Injection Analysis (FIA) method (Klunder et al., 2011). Filtered and acidified (Seastar© baseline hydrochloric acid; pH 1.7) seawater was concentrated on a column containing amino-di-acetic acid (IDA). Samples were analyzed in triplicate and standard deviations (SDs) are given. DFe concentrations ranged from 21 pM to 2.765 nM with the median at 0.124 nM. The mean SD of triplicate measurements was 2.7% of the DFe concentration. Blanks were determined daily by calculating the intercept of a seawater sample loaded for 0, 5 and 10 s. The blank values ranged from undetectable to 14 pM. The limit of detection of 16 pM was defined as 3 times the SD of the mean of the daily measured blanks.

The consistency of the FIA system over the course of a day was verified by measuring the same seawater sample several times. The observed drift was less than 5% and no corrections have been made for this drift. A certified SAFe standard (Johnson et al., 2007) for the long term consistency and absolute accuracy was measured on a regular basis (SAFe D2 (#94) 1.012 ± 0.015 nM Fe, $n = 9$; SAFe S (#173, 453, 87) 0.071 ± 0.010 nM Fe, $n = 18$).

2.2.2. Vertical turbulent eddy diffusivity estimates using CTD-data

CTD samples were obtained at a rate of 24 Hz. The average lowering speed was 0.4 m s^{-1}, so that measurements are made about every 0.017 m. During post-processing using SBE-software, potential surface-wave-influences, that may reverse direction of motion of the package, are filtered out by restricting to a CTD-speed of $>|0.25|$ m s^{-1}, whereby direction changes are removed. Corrections for thermal inertia of conductivity cells are applied and the data are transferred into 0.33 m vertical bins, thereby averaging some 20 data points per bin. This is consistent with the typical turbulent overturn-scale of 0.4 m that is resolvable using CTD-data (Stansfield et al., 2001). Ideally, it is preferred to use temperature-only data as a tracer for density to

compute turbulence parameters, under the condition of a tight T–S relationship. This holds not only in lakes, as in the original paper by Thorpe (1977), but also in the ocean, as CTD-computed density (anomaly) data are 3–10 times noisier than density from temperature alone (Stansfield et al., 2001; van Haren and Gostiaux, 2014). However, for polar regions where many salinity compensated intrusions exist (e.g. due to ice effects), the density data from the CTD is used to estimate turbulence parameters (Gargett and Garner, 2008).

The vertical turbulent eddy diffusivity (K_z) was estimated by calculating the 'Thorpe scale' (d_T) using the 0.33 m binned CTD-σ_θ (sigma-theta, density anomaly referenced to the surface) data. The parameter d_T is a vertical length scale of turbulent mixing in a stratified flow (Thorpe, 1977). It is obtained by rearranging an observed potential density profile, which may contain inversions associated with turbulent overturns, into a stable profile without inversions. The vertical displacement necessary to generate the stable profile is the 'Thorpe displacement'. A threshold of 0.0005 kg m^{-3} is used to discard apparent displacements associated with instrumental noise, as in Gargett and Garner (2008). These authors also propose to test for (a)symmetric distribution of positive and negative displacements to rule out spikes. In the present data, mostly obtained in good weather conditions, nearly all displacements passed this test, implying effective removal of spikes by the post-processing. Defining d_T as the root mean square of the Thorpe displacements within each turbulent overturn, the eddy diffusivity (m^2 s^{-1}) is obtained as:

$$K_z = 0.128 \ d_T^{\ 2} N \qquad (1)$$

where N denotes the buoyancy frequency and the constant 0.128 is derived from an empirical relation with the Ozmidov scale, the largest overturn scale in stratified waters, using a constant mixing efficiency of 0.2, which is typical for shear-induced turbulence (Dillon, 1982). The method of overturn displacements provides a reasonably adequate estimate of K_z and the turbulence dissipation rate to within a factor of

two, as has been established after comparison with independent estimates using free-falling microstructure data (e.g., Hosegood et al., 2005).

The raw $K_z(z)$ profiles were averaged in 50 m vertical bins, similar to the largest displacement observed, over which mean K_z values were calculated. When a BNL was present, a separate mean K_z was calculated for this layer and another for the water column between the BNL and the upper mixed layer, which was defined above the depth where the density was 0.02 kg m^{-3} higher than at the surface. At stations without a BNL, a single mean K_z value was calculated for the depth-range between the upper mixed layer and the deepest sample. The mean K_z values have a standard error of a factor of two times the mean and were used to calculate vertical fluxes. If a BNL was present, two fluxes were calculated, one over the steep DFe gradient from the BNL into the water just above the BNL and one from the water just above the BNL to the upper mixed layer. At these stations DFe gradients were calculated using mean values of DFe in the BNL, just above the BNL and in the upper mixed layer. If only one concentration was available for any of these layers, this concentration was used instead of a mean.

The horizontal turbulent fluxes of DFe from potential sources in the RSP were calculated using the horizontal turbulent diffusivity (K_h). To do this, the concentrations (C) of DFe (in nM m^{-3}) were fit exponentially to the equation:

$$C(x) = C_0 e^{-x/D} \qquad (1)$$

where C_0 is the concentration at the source, x is the distance from the source (m), and D is the scale length (m), defined as the distance where $C(x) = 0.37C_0$ (i.e. the concentration has decreased to 37% of the initial concentration). Once D was determined, we used the Okubo (1971) parameterization to estimate the K_h, (m^2 s^{-1}):

$$K_h = 7.3 \times 10^{-4} \ D^{1.15}, \qquad (2)$$

in which a 95% reduction length-scale l is used, $l = 3D$.

The horizontal turbulent flux (in nM m^2 s^{-1}) follows from:

$$F = K_h \partial C / \partial x, \qquad (3)$$

or:

$$F(x) = -7.3 \times 10^{-4} \ D^{0.15} C(x). \qquad (4)$$

3. Results

3.1. Water masses

Four main water masses can be distinguished in the Ross Sea, Antarctic Surface Water (AASW), Winter Water (WW), Shelf Water (SW), and Modified Circumpolar Deep Water (MCDW). AASW is defined by $\Theta > -1.85$ °C and neutral density <28 kg m^{-3} (Tomczak and Godfrey, 2001; Orsi and Wiederwohl, 2009), but shows a large variation in temperature and salinity. AASW is present as surface water throughout the Ross Sea, from which WW, defined by a temperature minimum as the remnant of the water mass formed during the previous winter under the warmer upper mixed layer, can be formed. WW was found in the central Ross Sea north of station 46, at stations 47, 49, 59 and 60 (Figs. 2B and C, 3D).

SW is formed near the RIS due to sea ice formation and melting. It is very cold ($\Theta < -1.85$ °C) and has variable salinity, depending on salt rejection processes. In the Ross Sea, SW can be divided into Ice Shelf Water (ISW) with $\Theta < -1.95$ °C, low salinity SW (LSSW with S <34.62), and high salinity SW (HSSW with S >34.62) (Orsi and Wiederwohl, 2009). ISW was recognized at stations 44 and 45 close to the RIS, where $\Theta < -2$ °C at depths of 253 and 227 m, respectively. Stations 49 and 61 were the most northern stations where SW, now Modified Shelf

Water (MSW), was present at the bottom (Fig. 2A–D). LSSW was found in the eastern Ross Sea and can be distinguished from the HSSW in the central and western Ross Sea by its lower salinity (Fig. 2A). In the western and central Ross Sea HSSW is flowing through the Drygalski and Joides Troughs towards the shelf break (Jacobs et al., 1970, 2002; Orsi and Wiederwohl, 2009) (Figs. 2B and C, 4E and D). SW flows cyclonically through the troughs to the shelf break, during which time it becomes MSW by mixing with the AASW and the incoming MCDW. MSW has characteristics between SW and Circumpolar Deep Water (CDW), with a broad range of salinities >34.5 and $\Theta > -1.85$ °C (Orsi and Wiederwohl, 2009).

Although Θ and S varied greatly in AASW, its salinity was always lower than the two deeper water masses, SW and CDW (Fig. 2). This was due to melting of the RIS in the south and to melting of sea ice elsewhere. The freshest AASW was found in surface waters of the Franklin Island transect at stations 87 and 90 (salinities of 33.9 and 34.0, respectively, Fig. 2D). Here, sea ice coverage was high (>50%), suggesting that the low salinity resulted from sea ice melt.

MCDW is characterized by a temperature maximum at depths between 200 and 400 m in the Ross Gyre (Jacobs et al., 2002) with a salinity between 34.5 and 35.0 and $\Theta > 0$ °C (Orsi and Wiederwohl, 2009). MCDW is formed at the shelf break where CDW flows onto the shelf from the north and mixes with SW and AASW, making MCDW colder and fresher, and therefore less dense, than CDW.

The presence of MCDW can be recognized in the Θ–S plots (Fig. 2B, C) and transect plots (Figs. 3, 4) by the elevated temperatures from mid-depth to the bottom. MCDW was located along the bottom as far south as 74.4°S between 175.7°E and 176.5°E; (between st. 61 and 63) and as far south as 75.5°S along 177.5°E (between st. 60 and 59). Further south, MCDW was found higher up in the water column, between MSW and AASW, and as far south as 76.75°S (between st. 46 and 47 along 177.55°E). The water properties at the Pennell Bank transect (Figs. 2C and 4) showed that the influence of MCDW, shown by the elevated Θ, decreased west of station 61. Apparently, MCDW entered this part of the Ross Sea Shelf predominantly over the Pennell Bank and on the eastern side of the Joides Trough.

3.2. DFe

In general, DFe was very low (0.02–0.08 nM) in the upper 100 m of the water column and increased with depth (Figs. 3A–6A, and Supplementary material Table 1). Low surface concentrations were observed in the AASW and WW (st. 47, 49–60), SW (st. 20, 30, 46, 85, 91 and 112) and occasionally extended into the MCDW (st. 60). The DFe concentrations were very low where phytoplankton biomass, as measured by fluorescence (Figs. 3–6), was high, suggesting biological DFe uptake. Low DFe waters (<0.1 nM) extended from the surface to 100 m depth in the southern RSP, close to the RIS (st. 44, 45, 46) and in the northwest (st. 75–91). In the central RSP and middle of the western RSP transect (st. 101–113), low DFe waters were found as deep as 200 m. At stations where deep waters had low DFe, phytoplankton biomass also extended deeper into the water column than at stations where low DFe was restricted closer to the surface.

Indications of DFe input at the surface from melting sea ice or dust deposition were only found at station 60, the only station in the RSP with relatively high surface DFe concentrations (0.18 nM DFe at 5 m and 0.20 nM DFe at 10 m depth). Also, the adjacent station 59 showed a small subsurface maximum of 0.1 nM DFe at 25 m depth, but no elevated surface DFe. Moreover, the upper 100 m of the Franklin Island transect with >50% sea ice cover only had slightly higher DFe concentrations than stations without sea ice (0.08 nM versus the mean of 0.06 nM with SD = 0.03, n = 114). In stations of the Franklin Island transect, DFe increased with depth from 0.06 nM at 10 m, 0.08–0.09 nM at 35 m and >0.1 nM at 100 m.

The potential of the RIS as a DFe source to the RSP was studied at stations nearby (st. 44 and 45). DFe maxima of 0.18 and 0.26 nM were
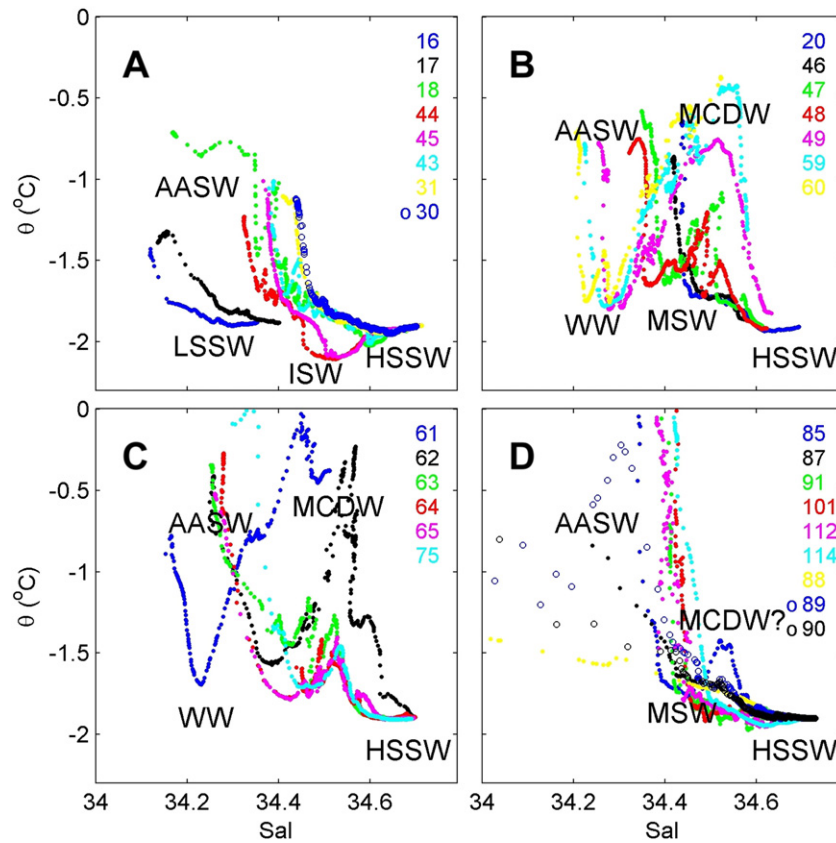
Fig. 2. Potential temperature (Θ)–salinity plots of all stations in the Ross Sea Polynya (RSP). Water masses indicated are: AntArctic Surface Water (AASW), Ice Shelf Water (ISW), Low Salinity Shelf Water (LSSW), High Salinity Shelf Water (HSSW), Modified Shelf Water (MSW), Circumpolar Deep Water (CDW), Modified Circumpolar Deep Water (MCDW), and Winter Water (WW). A: Eastern RSP (st. 16, 17) central RSP (st. 18 just east of central RSP transect, see Fig. 1) and the southern stations of the central RSP transect between the Ross Ice Shelf (RIS) and the Ross Bank (the legend of the stations is from south to north). B: Northern part of the central RSP transect, from the Ross Bank to Pennell Bank (st. 20–60 from south to north). C: Pennell Bank section (st. 61–75 from east to west). D: Western RSP transect including station 114 (st. 85–144 from north to south) and Franklin Island transect (st. 88–90 from east to west with st. 89 closest to Franklin Island).

found at a depth of 227 m at station 44 closest to the RIS and at 255 m at station 45, respectively (Fig. 7B). These maxima coincided with a distinct temperature minimum (below −2 °C), indicative of ISW (Fig. 3). The slightly elevated DFe of 0.15 nM at 120 m at station 43 (27.7 km to the north of st. 44) may be related to the outflow of ISW, (Θ = −1.88 °C). Our data show that the coincidence of maximum DFe and minimum temperature did not extend >30 km from the RIS.

The Franklin Island transect was sampled to study the importance of landmasses such as islands as a source of water column DFe. At depths between 75 and 400 m, DFe concentrations were indeed higher at the station closest to Franklin Island (st. 88) compared to the three stations further away (Fig. 7E), suggesting a potential subsurface source from Franklin Island. However, another source cannot be excluded.

In general, DFe increased with depth in the RSP, which is indicative of Fe sources from either deep water masses such as MCDW or the sediment. DFe in bottom waters near the sediments exhibited considerable variation throughout the study region (from 0.23 nM at 273 m at st. 60 to 2.76 nM at 753 m at st. 44), but we did not observe any spatial patterns with geographical location. For instance, DFe in bottom waters was relatively low, between 0.23 and 0.39 nM, at stations 44 and 45 near the RIS and station 60 on the Pennell Bank (0.39, 0.32 and 0.23 nM DFe, respectively). Intermediate concentrations between 0.5 and 0.7 nM DFe were observed at stations 46, 59, 85 and 101, and high concentrations up to 1.23–2.76 nM were measured at stations 43, 75 and 86. All stations with elevated DFe near the seafloor coincided with decreased transmissometer readings, indicative of a BNL (Figs. 3–6). At most stations with a BNL we observed an increase in DFe concentrations from ~6 to ~16 m above the sea floor. This feature was most distinct at station 114, where the BNL was sampled at three

depths and the highest DFe concentration was found in the upper sample 70 m from the bottom (Fig. 7F). Here, the reduced transmission indicative of a BNL reached 100 m from the seafloor.

At two stations south of 76°S in the central RSP (st. 20, 46) and at 77°S along the western RSP transect (st. 91), low transmission (93.6–98.2%) was found throughout the water column (Figs. 3, 6). This reduced transmission was not accompanied by enhanced fluorescence (<0.5 a.u.), suggesting that it was not caused by phytoplankton. At these stations, it appeared that fine suspended particles reached high enough concentrations throughout the water column to reduce transmission to the same degree as in a BNL. In contrast with a BNL, the reduced transmission was not associated with increased DFe. For example, station 20 exhibited relatively low and variable transmission over the entire water column, indicative of suspended particles, whereas station 45 did not show reduced transmission in the water column below the photic zone. However, the DFe depth profiles in the upper 200 m of both stations are similar (Fig. 7C).

4. Discussion

DFe was very low, on average 0.060 nM (SD = 0.028), throughout the upper 100 m of the water column of the RSP from December 20 to January 5, in general agreement with previous DFe measurements from the Ross Sea (Sedwick and DiTullio, 1997; Fitzwater et al., 2000; Coale et al., 2005; Sedwick et al., 2011; Marsay et al., 2014). DFe reached high concentrations at depth (mean 0.70 nM; SD = 0.58) as was also observed by Coale et al. (2005) and Marsay et al. (2014). The low DFe in surface waters suggests biological uptake of all bioavailable DFe by phytoplankton and an absence of Fe supply in excess of uptake by
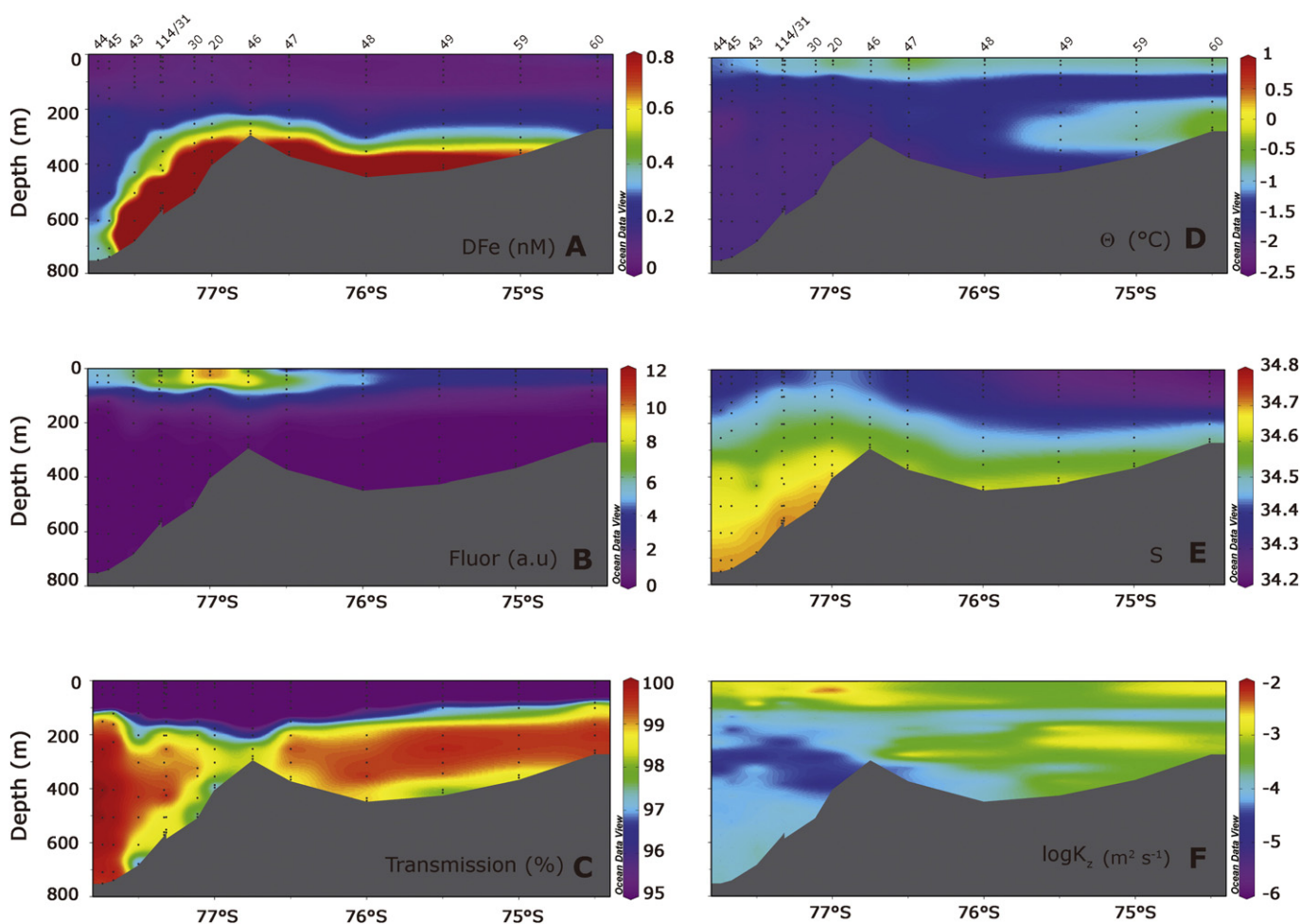
Fig. 3. Water properties along the south–north central Ross Sea Polynya transect from the Ross Ice Shelf at 77.74°S, 177.5°E at the left hand side to the north at the right hand side, crossing the Ross Trough to the Ross Bank, crossing a smaller trough to the Pennell Bank at 74.5°S, 177.5°E. Dots indicate the stations; station numbers are indicated. A: DFe in nM; B: CTD fluorescence in arbitrary units (a.u.), C: CTD transmission in % from 95 to 100; D: potential temperature Θ in °C; E: CTD salinity; F: logarithm of K_z in $m^2 s^{-1}$. St. 44 is north of the RIS, st. 44 and 45 are at the Ross Trough, st. 46 is at Ross Bank and st. 60 is at Pennell Bank.

phytoplankton. Our sampling period coincided with the annual early summer phytoplankton bloom in the RSP, with mean phytoplankton biomass in surface waters of 4.3 μg Chl a L^{-1} and primary productivity rates of 0.9 g C m^{-2} day^{-1} (Alderkamp, unpublished results). This phytoplankton productivity, despite the consistently low DFe in surface waters at levels considered to be growth limiting for phytoplankton (Timmermans et al., 2001, 2004; Garcia et al., 2009), suggests that Fe is being supplied to the phytoplankton bloom in the RSP throughout the growth season. Moreover, similarly low DFe in surface waters of the RSP was observed in early spring, from 16 November to 3 December 2006, before the peak of the phytoplankton bloom, (Sedwick et al., 2011), confirming DFe depletion very early in the growing season and the need for new sources of Fe to surface waters to sustain the phytoplankton bloom.

### 4.1. DFe requirements for phytoplankton blooms in the RSP

The RSP is the most productive Antarctic polynya, with the annual phytoplankton bloom usually beginning in early November and continuing through February. The bloom typically peaks in December when satellite observations show mean surface Chl a concentrations of 1.95 ± 0.86 μg L^{-1} (Arrigo and Van Dijken, 2003a). Mean in situ surface Chl a observations during December are even higher 4.97 ± 1.2 μg L^{-1} (Smith et al., 2003, 2006). We used the satellite derived mean Chl a of 1.95 μg L^{-1} from the December climatology for the RSP to calculate the DFe requirements of the phytoplankton during the

peak of the bloom in the RSP. We assumed a C:Chl a ratio of 100 g g^{-1} (Thompson et al., 1992) and an Fe:C ratio that ranges from 0.4 to 8.6 μmol·mol^{-1} (Strzepek et al., 2011), in agreement with the 6–14 μmol·mol^{-1} estimated by Twining et al. (2004) for natural phytoplankton populations under Fe-depleted conditions before Fe-enrichment during SOFEX. We calculated the Fe associated with phytoplankton to be 0.007 to 0.14 nM (μg Chl a L^{-1} × mg C:mg Chl a × mmol C:12 mg C × nmol Fe:mmol C − nmol Fe). Assuming an in situ phytoplankton growth rate of 0.13 day^{-1} (Alderkamp et al., unpublished data), and no remineralization of Fe from phytoplankton, the net flux of DFe necessary to sustain the observed phytoplankton bloom in an upper mixed layer of 50 m (average mixed layer depth) would be 0.4 to 9.1 × 10^{-7} mol Fe m^{-2} day^{-1} (0.007–0.14 × 10^{-9} mol Fe L^{-1} × 1000 = mol m^{-3} × 50 m = mol m^{-2} × 0.13 = mol m^{-2} day^{-1}). This is considered to be a minimum rate because it does not take into consideration potential losses of DFe due to coagulation, adsorption, precipitation, and sinking out of the upper mixed layer because quantifying these processes would be overly speculative.

4.2. Potential DFe sources to surface waters of the RSP

4.2.1. Vertical DFe fluxes from sediments

Vertical exchange and reductive dissolution of sediment are likely major DFe sources for the phytoplankton bloom in the RSP (Sedwick et al., 2011; De Jong et al., 2013; Marsay et al., 2014). We measured the highest DFe concentrations of all samples in the BNL, which was
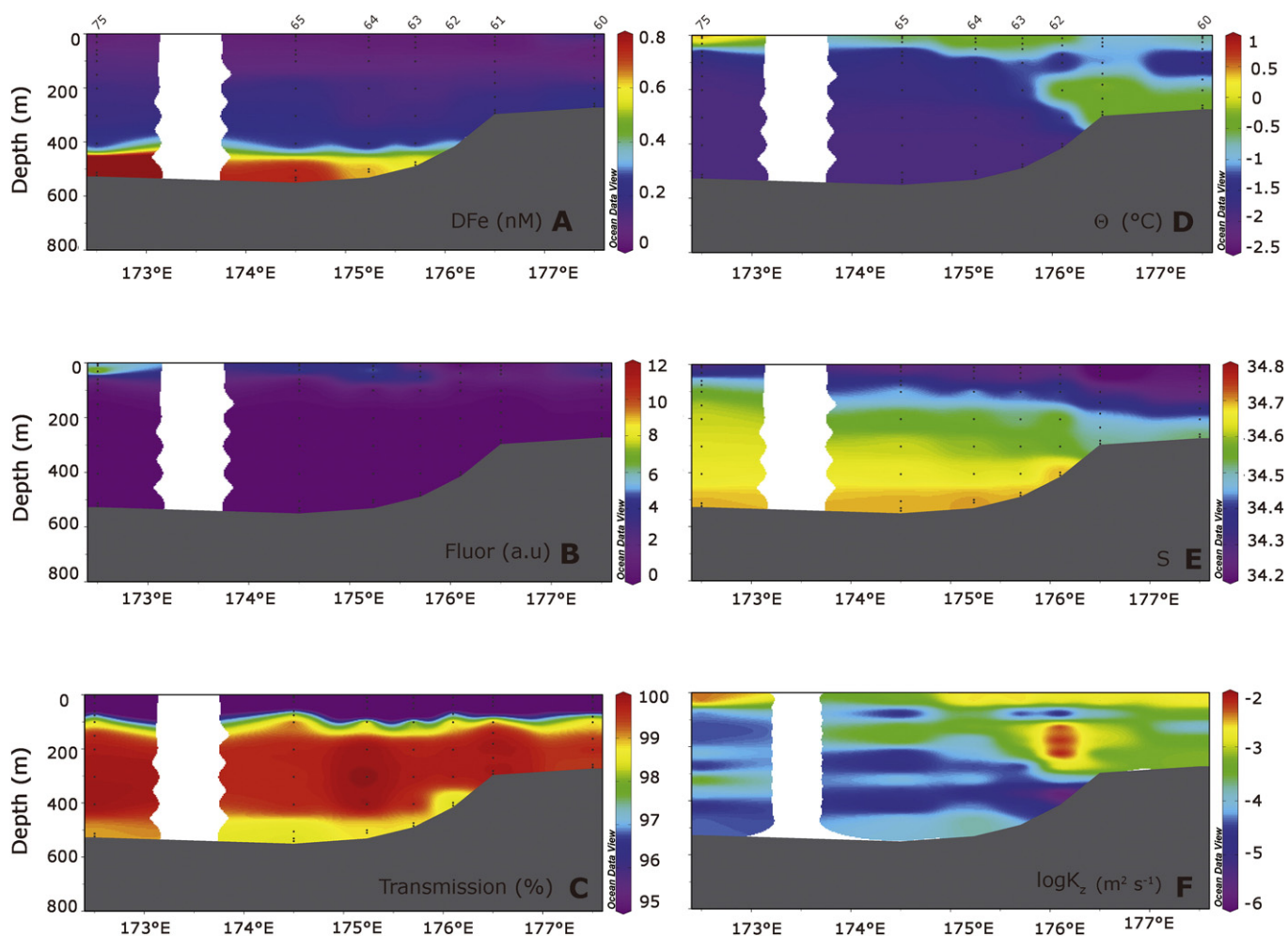
Fig. 4. Water properties of the east–west Pennell Bank transect from the Pennell Bank at 74.5°S, 177.5°E at the right hand side west to the Joides Trough at 74.5°S, 172.5°E at the left hand side. Dots indicate the stations; station numbers are indicated. A: DFe in nM; B: CTD fluorescence in arbitrary units (a.u.), C: CTD transmission in % from 95 to 100; D: potential temperature Θ in °C; E: CTD salinity; F: logarithm of K_z in m^2 s^{-1}.

present in almost all stations we sampled during the cruise (84%). This suggests that kinetic energy from currents, tidal movements, or internal waves was consistently high enough to resuspend sediments throughout the RSP (Dickson and McCave, 1986). Although, Marsay et al. (2014) observed a BNL at deeper stations in the RSP, during our study, neither deep stations 43 and 44 in the Ross Trough nor shallow stations 60 and 61 on the top of the Pennell Bank had a BNL. Whether the absence of a BNL was a transient or a permanent situation caused by low turbulence or a seafloor consisting of hard sediment or rock is not known. Generally, the BNL has a high potential to scavenge dissolved trace metals and thus low dissolved metal concentrations are expected (Bacon and Rutgers van der Loeff, 1989; Jeandel et al., 2015). However, recently, the release of metals from suspended sediments as a source of trace metals to the overlying waters has received more attention. Middag et al. (2011) and Klunder et al. (2012) showed a release of dissolved Mn (DMn) and DFe near the Arctic continental shelf from a nepheloid layer at intermediate depths. In addition, Hatta et al. (2013) measured elevated concentrations of dissolved Fe, Mn, and Al in Southern Ocean waters where resuspended sediments were detected near Drake Passage and concluded that resuspension plays an important role in enriching sea water with trace elements. Those findings are consistent with our observations of elevated DFe in the BNL.

DFe was often higher in the upper BNL and decreased with depth within the BNL (see Fig. 7F). This pattern may be an indication of the release of DFe from the seafloor sediments. Two potential processes releasing DFe from the sediment to the water include reductive

dissolution and sediment resuspension (a.o. Fitzwater et al., 2000; Sedwick et al., 2011; de Jong et al., 2013). If reductive dissolution is the main process for DFe release, the released dissolved FeII will oxidize in oxygenated waters to FeIII and will subsequently be precipitated and/or scavenged and sink out. Thus, DFe concentrations will decrease further from the source, which was not observed here. On the other hand, if the release is due to dissolution of DFe from resuspended particles, scavenging by slowly sinking particles will decrease DFe concentrations close to the seafloor, which was observed in the BNL. Dissolution of FeIII from resuspended sediment particles is only possible if dissolved organic ligands are unsaturated and can bind FeIII, which is the case here (unpublished results). In general, binding of FeIII by dissolved organic ligands increases the residence time of DFe in the water column which makes it more available for phytoplankton (Thuróczy et al., 2011; Gledhill and Buck, 2012).

To calculate the vertical diffusive DFe flux from the seafloor to the upper mixed layer where phytoplankton uptake occurs, we estimated the vertical turbulent eddy diffusivity (K_z) at every station. We divided the water column into an upper mixed layer of 50 m, a mid-depth layer with gradually increasing DFe with depth and, if present, a BNL in which DFe concentration was higher. At each station, we calculated the vertical gradients ($\partial DFe/\partial z$) between BNL and the water overlaying the BNL and between the water overlaying the BNL and the upper mixed layer. Mean K_z values were calculated for the layers in between (Fig. 8 and Supplementary material Table 2). At 84% of the stations, we obtained two DFe fluxes; one from the BNL (where present) to just above the BNL
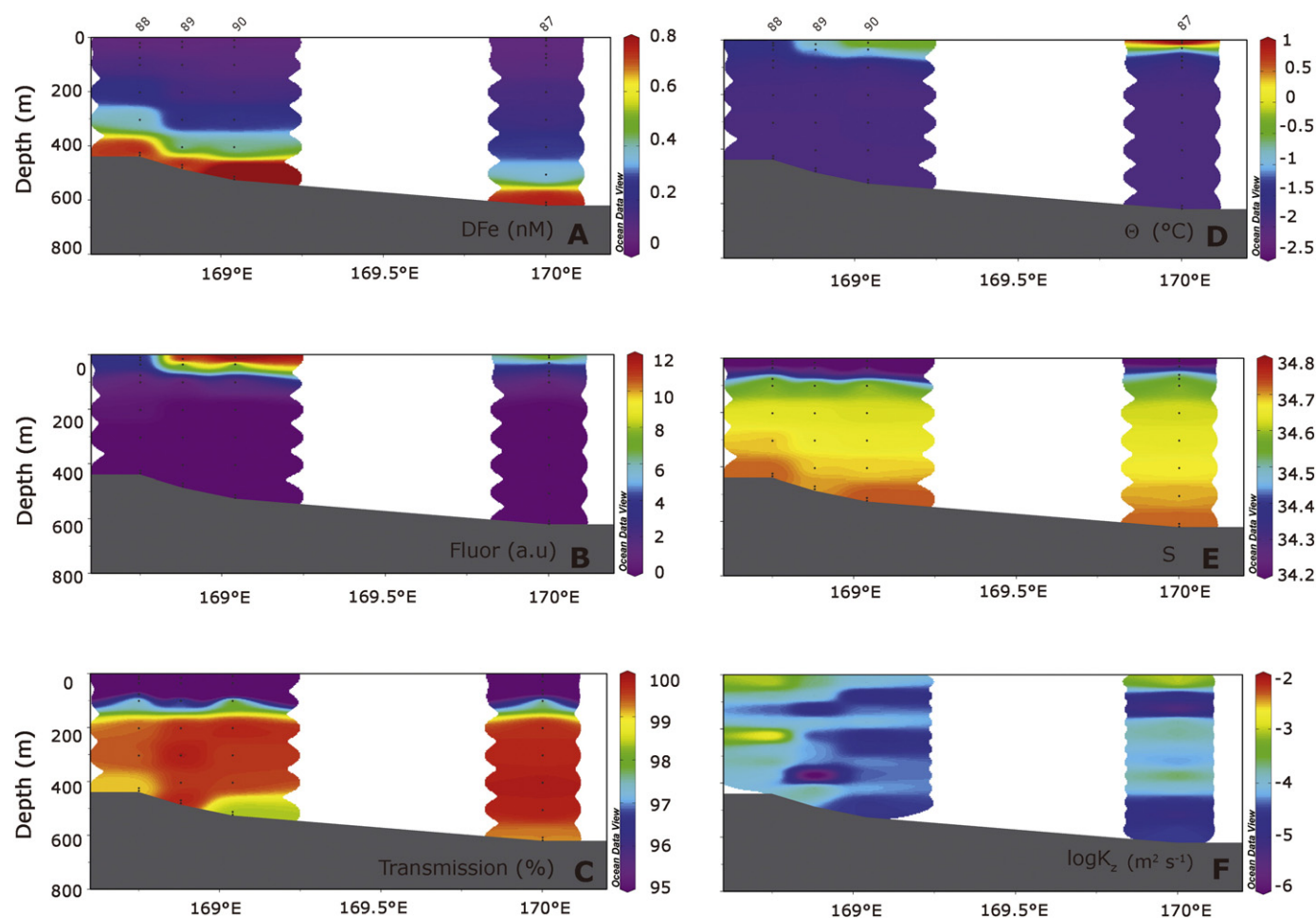
Fig. 5. Water properties of west–east Franklin Island transect from close to Franklin Island at 76.1°S, 168.7°E at the left hand side to 76.1°S, 170.2°E at the right hand side. Dots indicate the station samples; station numbers are indicated. A: DFe in nM; B: CTD fluorescence in arbitrary units (a.u.), C: CTD transmission in % from 95 to 100; D: potential temperature Θ in °C; E: CTD salinity; F: logarithm of K_z in $m^2 s^{-1}$.

where $\partial DFe/\partial z$ was strongest, and one from just above the BNL to the upper mixed layer. In the RSP DFe fluxes varied between 1.3×10^{-9} (st. 18) and 1.8×10^{-6} (st. 49) mol Fe m^{-2} day^{-1}. Since K_z was higher over the Ross and Pennell Banks (Figs. 3–5, Supplementary material Table 2), DFe fluxes were highest above slopes and tops of banks (Fig. 8). The mean vertical DFe fluxes at stations on banks (st. 20, 30, 46, 47, 48, 49, 59, 60, 61, 113) were 1.6×10^{-7} mol DFe m^{-2} day^{-1} for both fluxes and 0.8×10^{-7} mol DFe m^{-2} day^{-1} for the fluxes from just above the BNL to the upper mixed layer. These fluxes to the upper mixed layer are 0.1 to 2.0 times the calculated DFe flux needed to sustain the phytoplankton bloom. The mean DFe flux at stations in troughs is approximately a factor of two lower (3.3×10^{-8} mol Fe m^{-2} day^{-1}). Moreover, the importance of a BNL for the DFe flux to the upper mixed layer is illustrated comparing the DFe flux at bank station 60 without a BNL to the adjacent bank station 59 with a BNL and approximately the same water depth, where the DFe flux was approximately ten times higher. Marsay et al. (2014) used a regional circulation model of the Ross Sea to estimate K_z values used for calculation of vertical DFe fluxes. Comparison of their model K_z with our in situ K_z estimates shows that our in situ median K_z is approximately a factor of 10 smaller than the model K_z, which suggests a reasonably good agreement of the two methods considering that the values range over four orders of magnitude. However, the spatial variation of our K_z is a factor of 10^3 larger than the modeled K_z, suggesting greater natural variability in K_z than what is produced by a regional model. The mean K_z values in the BNL were 3.2 times lower than those between the BNL and upper mixed layer, showing that separating

the water column below the upper mixed layer into two layers based on the presence of a BNL is useful for calculations of both the vertical DFe gradient ($\partial DFe/\partial z$) and K_z. The benthic DFe fluxes calculated by Marsay et al. (2014) from the sediment to 200 m depth, using their higher model K_z values, are more than 10 times higher than our fluxes, ranging from 2.8×10^{-8}–8.2×10^{-6} mol DFe m^{-2} day^{-1}, with a geometric mean of 3.7×10^{-7} mol DFe m^{-2} day^{-1}. Our values range from 1.3×10^{-9} to 1.8×10^{-6} mol DFe m^{-2} day^{-1} with a geometric mean from the BNL to the layer just above of 3.3×10^{-8} mol DFe m^{-2} day^{-1}. These flux estimates are at the lower range of published vertical flux estimates (Gerringa et al., 2012; Marsay et al., 2014 and references therein).

4.2.2. Horizontal DFe fluxes from banks

Sediments from banks act as DFe sources to subsurface waters via horizontal transport (Sedwick et al., 2011; De Jong et al., 2013). However, we observed no subsurface DFe trends with distance from either the Ross Bank (Fig. 3A) or the Pennell Bank (Fig. 4A). Thus, there were no indications that the banks were significant DFe sources to deep waters in the Ross Sea via horizontal transport, despite the fact that the vertical DFe fluxes over the banks were high (Fig. 7C and D).

4.2.3. Horizontal DFe fluxes from landmasses

Horizontal DFe transport from Franklin Island was studied to understand the importance of landmasses as DFe source to the Ross Sea. Indeed, in the Franklin Island transect, DFe concentration below 100 m depth decreased with distance from Franklin Island (Fig. 7E). No
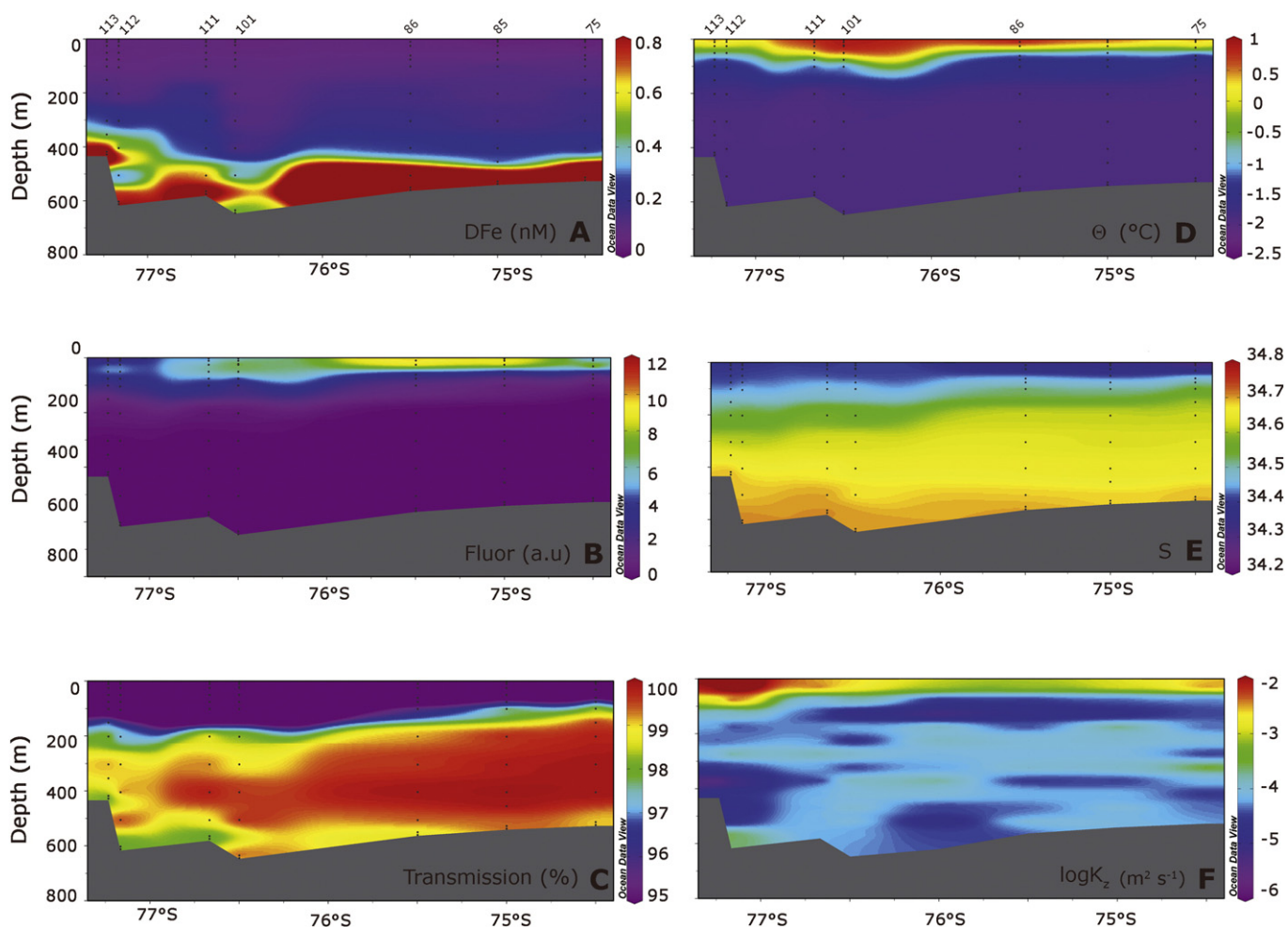
Fig. 6. Water properties of western Ross Sea Polynya transect, the north–south transect from station 75 (74.5°S, 172.5°E) at the right hand side to the south-west to station 101 (76.5°S, 171°E) and from there to the south-east to station 113 (77.33°S, 177.5°E) at the left hand side which has the same position as station 31 of the central Ross Sea transect. Dots indicate the station samples; station numbers are indicated. A: DFe in nM; B: CTD fluorescence in arbitrary units (a.u.), C: CTD transmission in % from 95 to 100; D: potential temperature Θ in °C; E: CTD salinity; F: logarithm of K_z in $m^2 s^{-1}$.

decrease was detected in surface waters (<100 m), since DFe was low at all stations (Fig. 9), presumably due to phytoplankton uptake, as suggested by the high fluorescence in surface waters. Since there was no horizontal DFe gradient in surface waters, we cannot calculate a horizontal DFe flux. In addition, horizontal DFe trends could not be obtained in deep waters below 400 m since at this depth the distance to the BNL determines the DFe concentration. However, we observed a decrease in DFe with distance from Franklin Island at depths of 200 m and 300 m that we fitted exponentially to obtain the scale length over which the DFe concentration at the source (C_0) is reduced to 0.37C_0. The calculated scale lengths are 125 and 60 km for 200 and 300 m depth, respectively. These scale lengths are in agreement with published scale lengths of 16 km for surface waters in Monterey Bay (Johnson et al., 1997), 25 km for the surface waters near Crozet Island and near the Antarctic Peninsula (Planquette et al., 2007, Ardelan et al., 2010), 59 km for waters at 100 m depth in the Pine Island Polynya (Gerringa et al., 2012), and 131 km for water at 40 m depth near the Kerguelen Islands (Bucciarelli et al., 2001).

The scale lengths obtained here near Franklin Island result in horizontal fluxes at 200 m of 5.5 and 2.6×10^{-5} mol DFe m^{-2} day^{-1} and at 300 m of 5.0 and 3.4×10^{-5} mol DFe m^{-2} day^{-1} at distances of 50 and 100 km from Franklin Island, respectively. To compare the transport of DFe via horizontal flux (F_h) with the supply needed to sustain phytoplankton growth in the upper mixed layer, and with the vertical transport, we converted the net F_h fluxes into units of volume. We calculated the horizontal fluxes at 200 m depth at distances of 50 and

100 km from Franklin Island and assumed the first flux to be the influx and the second flux to represent the outflux from a box over the 50 km distance difference. The difference between these fluxes divided by the distance between in- and outflux is the net horizontal flux or transport of DFe ((F_h(50 km) − F_h(100 km)) / 50 km). This results in a net flux of 3.3 to 5.8×10^{-10} mol DFe m^{-3} day^{-1}. Since the vertical DFe-transport is calculated to the upper 50 m, the average MLD, we divided the vertical transport by 50, to compare both fluxes in the same units. This resulted in vertical diffusive fluxes of 6.7 to 4.3×10^{-10} mol DFe m^{-2} day^{-1} (using 3.3×10^{-8} mol DFe m^{-2} day^{-1}, which is the mean for all the fluxes from just above the BNL to the upper mixed layer, and 2.1×10^{-8} mol DFe m^{-2} day, which is the mean of the fluxes for stations 88–90 near Franklin Island from Supplementary material Table 2). This calculation shows that at a horizontal distance between 50 and 100 km from the source the horizontal transport at 200 m depth is approximately the same as the mean vertical transport, suggesting that the horizontal DFe flux from landmasses can be important. However, vertical transport is needed to bring DFe up to the phytoplankton in the upper mixed layer and this process likely becomes the determining factor for transport up to the phytoplankton in the upper mixed layer.

### 4.2.4. Horizontal DFe fluxes from the Ross Ice Shelf

We did not discern horizontal trends in DFe with distance from the RIS at any depth of the water column (Figs. 3A, 7B and C; Supplementary
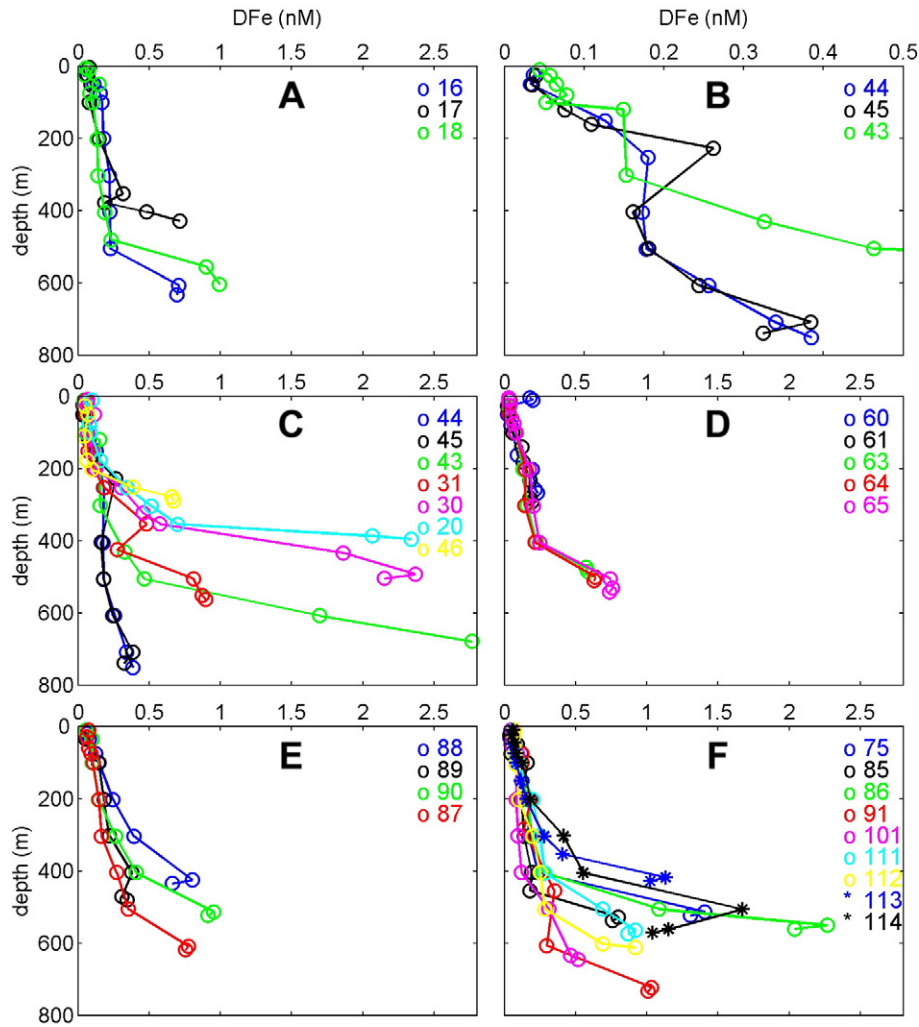
Fig. 7. DFe (nM) depth profiles, highlighting specific features explained in the text (data is in Supplementary material Table 1). A: stations 16 and 17 from the eastern Ross Sea Polynya (RSP) and station 18 east of the central transect (see Fig. 1), these stations are not shown in the transects (Figs. 3–6). B: stations 44, 45 and 43 at the southern end of the central RSP transect close to the Ross Ice Shelf (RIS) (transect in Fig. 3). Scale is cut off at 0.5 nM to show the elevated DFe in Intermediate Shelf Water (ISW). The deep samples of st. 43 falls outside the plotted range, see panel C for the full profile. C: stations at the southern end of the central RSP transect from the RIS Trough to the Ross Bank (incl station cut-off in B). D: stations from Pennell Bank transect to the Joides Trough. E: stations at the Franklin Island transect. F: stations from the western RSP transect showing that in stations where the Bottom Nepheloid Layer (BNL) was sampled (e.g. st. 86, 113, 114) DFe decreased towards the seafloor and the highest DFe was found at some distance from the seafloor.

material Table 1) and therefore, a horizontal DFe flux from the RIS to the RSP could not be calculated. According to observations by Jacobs et al. (1970), and Jacobs and Giulivi (1998), and modeling by Holland et al. (2003), the main outflow of ISW from under the RIS is located just west of 180° where stations 43–45 were located (Fig. 2B). The ISW distinguished at stations 44 and 45 contained slightly elevated DFe (Fig. 7B), indicating that the RIS may be a small DFe source. However,

our data suggest that the elevated DFe in ISW does not reach far into the polynya. At greater distances from the RIS, the ISW forms SW, in which no elevated DFe was detected. Therefore, we conclude that DFe in ISW is not a significant DFe source for the RSP, in contrasts with the previous suggestions (Fitzwater et al., 2000; Sedwick et al., 2000). In
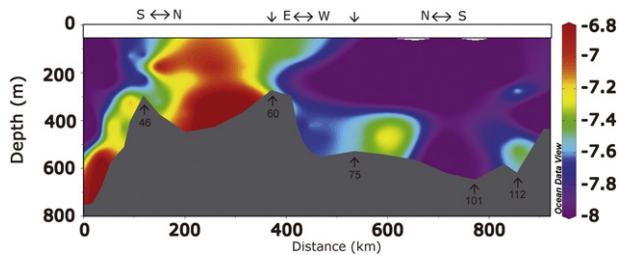
Fig. 8. The logarithm of the vertical diffusive fluxes of Fe (mol m^{-2} day^{-1}) to the upper mixed layer (50 m) calculated for the circle transect. This transect is the connection of the central RSP, Pennell Bank and Western RSP transects (Fig. 1). Arrows indicate the position where transects (Figs. 3, 4 and 6) connect and change direction. The Franklin Island transect is not part of this figure.
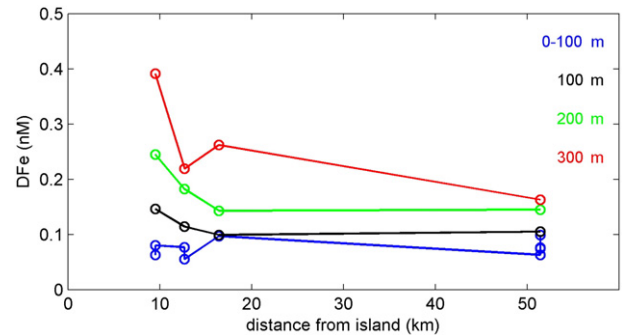
Fig. 9. DFe for different depth ranges as a function of the distance to Franklin Island at stations 88 (9.5 km), 89 (12.7 km), 90 (16.5 km) and 87 (51.4 km). The exponential equations fitted to the decrease with distance are f(x) = 0.2083e$^{-0.008}$, and f(x) = 0.3457 e$^{-0.015}$, at 200 m, and 300 m, respectively. R^2 being 0.3719, and 0.6466, respectively.

contrast to the RIS, the Pine Island Glacier was found to be the main source of DFe to the phytoplankton bloom in the Pine Island Polynya (Gerringa et al., 2012). An important difference between these two glaciers is the size of the cavity below the floating glacier terminus and the direct access of the relatively warm MCDW that drives basal melt in the Pine Island Glacier (Jacobs et al., 2011). The cavity under the RIS is much larger than that under the Pine Island Glacier and during the long time that the ice sheet is transported over this cavity, the bottom of the floating ice tongue is slowly melting and, releasing its Fe into the water. Here, particles may sink and DFe may aggregate and sink out of the water column. Moreover, the basal melt rate of the RIS is smaller than that of the Pine Island Glacier (Rignot et al., 2013). We did not observe any hints of particle outflow from under the RIS as the transmission in waters below the euphotic zone close to the RIS was near 100%.

4.2.5. DFe fluxes from deep water masses

CDW has elevated DFe compared to AASW (Klunder et al., 2011; Sedwick et al., 2011) and may thus be a DFe source to surface waters. CDW may be a direct DFe source to the RSP (Sedwick et al., 2011) and/or MCDW may be enriched with DFe from sediments as it flows over the shelf (Gerringa et al., 2012). MCDW was only observed as a deep water mass in the northern Ross Sea, at stations 60 and 61. This MCDW had low DFe (0.20 and 0.23 nM at st. 60 and 61, respectively), even though it had already traveled over the seafloor from the shelf break. Thus, MCDW does not appear to be a DFe source to the RSP. In fact, stations 60 and 61 have the lowest DFe in the deepest sample of all stations in the RSP.

4.2.6. Sea ice

DFe may accumulate in sea ice, either due to atmospheric dust deposition over time (Sedwick et al., 2011; De Jong et al., 2013) or remineralization of particulate Fe from ice algae by the heterotrophic activity of bacteria and protozoa within the ice (Sedwick and DiTullio, 1997; Lannuzel et al., 2010, 2014; van der Merwe et al., 2011). This DFe is released in surface waters when the sea ice melts (Sedwick et al., 2011; De Jong et al., 2013). In general dust is not considered to be an important source of DFe for the nearshore waters of Antarctica (Martin et al., 1990). Atmospheric dust quantities in the Southern Ocean are among the lowest in the world (Duce and Tindale, 1991). However, the Ross Sea may be an exception due to the proximity of sources of windblown particles such as the McMurdo Ice Shelf, the Dry Valleys, Ross Island, and Erebus volcanic emissions. Thus, atmospheric dust deposition may be an important DFe source for sea ice in the Ross Sea (Sedwick et al., 2011; De Jong et al., 2013).

We sampled only four stations with a considerable sea ice cover in the northern RSP and the Franklin Island transect. Elevated DFe in surface waters was only observed at one of these stations, in the northern RSP (st. 60; Fig. 7D). We used the turbulent eddy diffusivity coefficient K_z (see below) to calculate the downward transport of DFe released from sea ice in the upper 10 m (at station 60) to waters into the upper mixed layer below. This DFe flux from 10 m depth into the mixed layer (10–56 m) was 5.6×10^{-7} mol DFe m^{-2} day^{-1}, which is 0.2–4 times the DFe flux necessary to sustain the phytoplankton bloom. The other three stations with sea ice coverage >50% were near Franklin Island and did not show elevated DFe (within the SD of the mean DFe) in surface waters, suggesting either that there was no DFe input from melting sea ice or that it was immediately taken up by phytoplankton. Our data show that sea ice may be a considerable DFe source locally, but this effect was spatially highly variable. Although DFe from sea ice may play an important role during the opening of the polynya and at the edges of the polynya, once it is open, the effect is negligible in the RSP.

4.2.7. Icebergs

Icebergs may be a DFe source to surface waters which on occasion may be important to the RSP (De Baar et al., 1995; Sedwick et al., 2011). However, they can also be the cause of a reduction in primary production in the RSP. In 2000 and in 2002, enormous icebergs (B-15 and C-19, respectively) did calve off the front of the Ross Ice Shelf and prevented sea ice from advecting out of the Ross Sea Polynya. The polynya was much smaller than normal and primary production was greatly reduced (Arrigo and Van Dijken, 2003b). Since we did not encounter any icebergs in the RSP during the NBP 13-10 cruise, they cannot be considered here.

5. Conclusions

DFe concentrations in surface waters (<100 m depth) of the RSP were low (<0.1 nM) during early summer, coinciding with the annual phytoplankton spring–summer bloom. DFe concentrations increased with depth to 0.2–0.4 nM in deeper waters. The highest DFe concentrations (up to 2.7 nM) were found within BNLs near the seafloor. At the few stations where no BNL was present, DFe near the seafloor was lower.

Our investigation shows that during early summer the main DFe source to the phytoplankton bloom was the vertical diffusive DFe transport from the seafloor sediments to the upper mixed layer. The mean vertical DFe flux from waters above the BNL to the upper mixed layer was 3.3×10^{-8} mol DFe m^{-2} day^{-1}. The greatest vertical DFe fluxes were observed above sediments with a BNL. In addition, vertical DFe fluxes were high above banks and slopes due to the smaller distance to the source and to the larger K_z, reflecting greater turbulence. Stations near Franklin Island showed that a horizontal flux from a landmass such as an island can be a substantial DFe source to deep waters (<200 m depth). However, in early summer, when we sampled, no transport from Franklin Island could be detected in the upper 100 m. A horizontal gradient in DFe from the island was observed only at 200 and 300 m depth and the net transport at a distance between 50 and 100 km from the source was of the same magnitude as the vertical flux. However, a mechanism for vertical transport is needed to bring this DFe to the upper mixed layer where it may support primary productivity. We found no indication that the RIS is a significant DFe source to the RSP, although we observed slightly elevated DFe in ISW (0.18 and 0.26 nM) when compared to surrounding waters (0.12–0.15 nM). Sea ice was a minor DFe source near Franklin Island. Only at one station in the marginal sea ice zone in the north of the polynya did we find sea ice to be a sufficient DFe source to fuel the phytoplankton biomass levels that were present.

The finding that the vertical diffusive DFe flux was the main DFe source to the upper mixed layer in the RSP suggests that the continental shelf width is an important feature supporting DFe flux to the surface and supporting primary productivity. A wide shelf, such as in the Ross Sea, provides a large area where exchange of DFe occurs, which can lead to a substantial DFe flux to surface waters. However, our study shows that the vertical diffusive DFe flux can vary by an order of magnitude between different stations, suggesting that local conditions, such as the presence of a BNL and turbulence that enhances K_z, greatly affect DFe fluxes to the upper mixed layer. Moreover, bathymetric features such as the Ross and Pennell Banks greatly enhanced the vertical diffusive DFe flux, which is also expected to be high over the Mawson Bank in the northwest RSP. Strikingly, satellite studies have revealed that the phytoplankton biomass during the Austral summer (January and February) towards the end of the growing season is higher over the Pennell and Mawson Banks (e.g. Reddy and Arrigo, 2006; Smith et al. 2012). This suggests that the high vertical DFe fluxes over the banks are a permanent feature in the RSP that supports phytoplankton productivity.

Supplementary data to this article can be found online at http://dx.doi.org/10.1016/j.marchem.2015.06.002.

References

Ainley, D.G., Ballard, G., Dugger, K.M., 2006. Competition among penguins and cetaceans reveals trophic cascades in the western Ross Sea, Antarctica. Ecology 87, 2080–2093.

Alderkamp, A.-C., Mills, M.M., van Dijken, G.L., Laan, P., Thuróczy, C.-E., Gerringa, L.J.A., de Baar, H.J.W., Payne, C., Tortell, P., Visser, R.J.W., Buma, A.G.J., Arrigo, K.R., 2012. Iron from melting glaciers fuels phytoplankton blooms in Amundsen Sea (Southern Ocean): phytoplankton characteristics and productivity. Deep-Sea Res. II 71–76, 32–48.

Alderkamp, A.C., Van Dijken, G.L., Lowry, K.E., Connelly, T.L., Lagerström, M., Sherrell, R.M., Haskins, C., Rogalsky, E., Schofield, O., Stammerjohn, S.E., Yager, P.L., Arrigo, K.R., 2015. Fe availability drives photosynthesis rates during the build-up phase of the phytoplankton bloom in the Amundsen Sea Polynya, Antarctica. Elementa: Science of the Anthropocene 3, 00043.

Aquilina, A., Homoky, W.B., Hawkes, J.A., Lyons, T.W., Mills, R.A., 2014. Hydrothermal sediments are a source of water column Fe and Mn in the Bransfield Strait, Antarctica. Geochim. Cosmochim. Acta 137, 64–80.

Ardelan, M.V., Holm-Hansen, O., Hewes, C.D., Reiss, C.S., Silva, N.S., Dulaiova, H., Steinnes, E., Sakshaug, E., 2010. Natural iron enrichment around the Antarctic Peninsula in the Southern Ocean. Biogeosciences 7, 11–25.

Arrigo, K.R., van Dijken, G.L., 2003a. Phytoplankton dynamics within 37 Antarctic coastal polynya systems. J. Geophys. Res. 108 (C8), 3271. http://dx.doi.org/10.1029/2002JC001739.

Arrigo, K.R., van Dijken, G.L., 2003b. Impact of iceberg C-10 on Ross Sea primary production. Geophys. Res. Lett. 30, 1836. http://dx.doi.org/10.1029/2003GL017721.

Arrigo, K.R., van Dijken, G.L., 2004. Annual changes in sea ice, chlorophyll a, and primary production in the Ross Sea, Antarctica. Deep-Sea Res. II 51, 117–138.

Arrigo, K.R., Worthen, D.L., Robinson, D.H., 2003. A coupled ocean-ecosystem model of the Ross Sea. Iron regulation of phytoplankton taxonomic variability and primary production. J. Geophys. Res. 108, 3231. http://dx.doi.org/10.1029/2001JC000856.

Arrigo, K.R., van Dijken, G.L., Bushinsky, S., 2008a. Primary production in the Southern Ocean, 1997–2006. J. Geophys. Res. 113, C08004. http://dx.doi.org/10.1029/2007JC004551.

Arrigo, K.R., van Dijken, G., Long, M., 2008b. Coastal Southern Ocean: a strong anthropogenic CO₂ sink. Geophys. Res. Lett. 35, L21602. http://dx.doi.org/10.1029/2008GL035624.

Bacon, M.P., Rutgers van der Loeff, M.M., 1989. Removal of thorium-234 by scavenging in the bottom nepheloid layer of the ocean. Earth Planet. Sci. Lett. 92, 157–164.

Blain, S., Quéguigiener, B., Armand, L., Belviso, S., Bombled, B., Bopp, L., Bowie, A., Brunet, C., Brussaard, C., Carlotti, F., Christaki, U., Corbière, A., Durand, I., Ebersbach, F., Fuda, J.-L., Garcia, N., Gerringa, L., Griffiths, B., Guigue, C., Guillerm, C., Jacquet, S., Jeandel, C., Laan, P., Lefèvre, D., Lomonaco, C., Malits, A., Mosseri, J., Obernosterer, I., Park, Y.-H., Picheral, M., Pondaven, P., Remenyi, T., Sandroni, V., Sarthou, G., Savoye, N., Scouarnec, L., Souhaut, M., Thuiller, D., Timmermans, K., Trull, T., Uitz, J., van-Beek, P., Veldhuis, M., Vincent, D., Viollier, E., Vong, L., Wagener, T., 2007. The effect of natural iron fertilization on carbon sequestration in the Southern Ocean. Nature 446, 1070–1075.

Blain, S., Sarthou, G., Laan, P., 2008. Distribution of dissolved iron during the natural iron fertilisation experiment KEOPS (Kerguelen Plateau, Southern Ocean). Deep-Sea Res. II 55, 594–605.

Bowie, A.R., van der Merwe, P., Quéroué, F., Trull, T., Fourquez, M., Planchon, F., Sarthou, G., Chever, F., Townsend, A., Obernosterer, I., Blain, S., 2014. Iron budgets for three distinct biogeochemical sites around the Kerguelen archipelago (Southern Ocean) during the natural fertilization experiment KEOPS-2. Biogeosciences 11, 17861–17923. http://dx.doi.org/10.5194/bgd-11-17861-2014.

Boyd, P.W., Jickells, T., Law, C.S., Blain, S., Boyle, E.A., Buesseler, K.O., Coale, K.H., Cullen, J.J., De Baar, H.J.W., Follows, M., Harvey, M., Lancelot, C., Levasseur, M., Owens, N.P.J., Pollard, R., Rivkin, R.B., Sarmiento, J., Schoemann, V., Smetacek, V., Takeda, S., Tsuda, A., Turner, S., Watson, A.J., 2007. Mesoscale iron enrichment experiments 1993–2005: synthesis and future directions. Science 315, 612–617.

Boyd, P.W., Arrigo, K.R., Strzepek, R., van Dijken, G.L., 2012. Mapping phytoplankton iron utilization: insights into Southern Ocean supply mechanisms. J. Geophys. Res. 117, C06009. http://dx.doi.org/10.1029/2011JC007726.

Boye, M., van den Berg, C.M.G., de Jong, J.T.M., Leach, H., Croot, P.L., de Baar, H.J.W., 2001. Organic complexation of iron in the Southern Ocean. Deep-Sea Res. I 48, 1477–1497.

Bucciarelli, E., Blain, S., Tréguer, P., 2001. Iron and manganese in the wake of the Kerguelen Islands (Southern Ocean). Mar. Chem. 73, 21–36.

Coale, K.H., Gordon, R.M., Wang, X., 2005. The distribution and behavior of dissolved and particulate iron and zinc in the Ross Sea and Antarctic circumpolar current along 170°W. Deep-Sea Res. I 52, 295–318.

Croot, P.L., Andersson, K., Öztürk, M., Turner, D.R., 2004. The distribution and speciation of iron along 6°E in the Southern Ocean. Deep-Sea Res. II 51, 2857–2879.

Croot, P.L., Frew, R.D., Sander, S., Hunter, K.A., Ellwood, M.J., Pickmere, S.E., Abraham, E.R., Law, C.S., Smith, M.J., Boyd, P.W., 2007. Physical mixing effects on iron biogeochemical cycling: FeCycle experiment. J. Geophys. Res. 112, C06015. http://dx.doi.org/10.1029/2006JC003748.

de Baar, H.J.W., Buma, A.G.J., Nolting, R.F., Cadée, G.C., Jacques, G., Tréguer, P.J., 1990. On iron limitation of the Southern Ocean: experimental observation in the Weddell and Scotia Seas. Mar. Ecol. Prog. Ser. 65, 105–122.

De Baar, H.J.W., de Jong, J.T.M., Bakker, D.C.E., Löscher, B.M., Veth, C., Bathmann, U., Smetacek, V., 1995. Importance of iron for phytoplankton spring blooms and CO₂ drawdown in the Southern Ocean. Nature 373, 412–415.

De Baar, H.J.W., Boyd, P.W., Coale, K.H., Landry, M.R., Tsuda, A., Assmy, P., Bakker, D.C.E., Bozec, Y., Barber, R.T., Brzezinski, M.A., Buesseler, K.O., Boye, M., Croot, P.L., Gervais, F., Gorbunov, M.Y., Harrison, P.J., Hiscock, W.T., Laan, P., Lancelot, C., Law, C.S., Levasseur, M., Marchetti, A., Millero, F.J., Nishioka, J., Nojiri, Y., van Oijen, T., Riebesell, U., Rijkenberg, M.J.A., Saito, H., Takeda, S., Timmermans, K.R., Veldhuis, M.J.W., Waite, A.M., Wong, C.S., 2005. Synthesis of iron fertilization experiments: from the iron age in the age of enlightenment. J. Geophys. Res. 110, C09S16. http://dx.doi.org/10.1029/2004JC00260.

de Jong, J., Schoemann, V., Lannuzel, D., Croot, P., De Baar, H., Tison, J.-L., 2012. Natural iron fertilization of the Atlantic sector of the Southern Ocean by continental shelf sources of the Antarctic Peninsula. J. Geophys. Res. 117, G01029. http://dx.doi.org/10.1029/2011JG001679.

de Jong, J., Schoemann, V., Maricq, N., Mattielli, N., Langhorne, P., Haskell, T., Tison, J.-L., 2013. Iron in land-fast sea ice of McMurdo Sound derived from sediment resuspension and wind-blown dust attributes to primary productivity in the Ross Sea, Antarctica. Mar. Chem. 157, 24–40.

Dickson, R.R., McCave, I.N., 1986. Nepheloid layers on the continental slope west of Porcupine Banks. Deep-Sea Res. 33, 791–818.

Dillon, T.M., 1982. Vertical overturns: a comparison of Thorpe and Ozmidov length scales. J. Geophys. Res. 87, 9601–9613.

Duce, R.A., Tindale, N.W., 1991. Atmospheric transport of iron and its deposition in the ocean. Limnol. Oceanogr. 36, 1715–1726.

Fitzwater, S.E., Johnson, K.S., Gordon, R.M., Coale, K.H., Smith Jr., W.O., 2000. Trace metal concentrations in the Ross Sea and their relationship with nutrients and phytoplankton growth. Deep-Sea Res. II 47, 3159–3179.

Garcia, N.S., Sedwick, P.N., DiTullio, G.R., 2009. Influence of irradiance and iron on the growth of colonial Phaeocystis antarctica: implications for seasonal bloom dynamics in the Ross Sea, Antarctica. Aquat. Microb. Ecol. 57, 203–220. http://dx.doi.org/10.3354/ame01334.

Gargett, A., Garner, T., 2008. Determining Thorpe scales from ship-lowered CTD density profiles. J. Atmos. Ocean. Technol. 25, 1657–1670.

Gerringa, L.J.A., Blain, S., Laan, P., Sarthou, G., Veldhuis, M.J.W., Brussaard, C.P.D., Viollier, E., Timmermans, K.R., 2008. Fe-containing dissolved organic ligands near the Kerguelen Archipelago in the Southern Ocean (Indian sector). Deep-Sea Res. II 55, 606–621.

Gerringa, L.J.A., Alderkamp, A.-C., Laan, P., Thuróczy, C.-E., De Baar, H.J.W., Mills, M.M., van Dijken, G.L., van Haren, H., Arrigo, K.R., 2012. Iron from melting glaciers fuels the phytoplankton blooms in Amundsen Sea (Southern Ocean): iron biogeochemistry. Deep-Sea Res. II 71–76, 16–31.

Gledhill, M., van den Berg, C.M.G., 1994. Determination of complexation of iron(III) with natural organic complexing ligands in seawater using cathodic stripping voltammetry. Mar. Chem. 47, 41–54.

Gledhill, M., Buck, K.N., 2012. The organic complexation of iron in the marine environment: a review. Frontiers in microbiology http://dx.doi.org/10.3389/fmicb.2012.00069.

Hassler, C.S., Alasonati, E., Mancuso Nichols, C.A., Slaveykova, V.I., 2011. Exopolysaccharides produced by bacteria isolated from the pelagic Southern Ocean - Role in Fe binding chemical reactivity, and bioavailability. Mar. Chem. 123, 88–98.

Hatta, M., Measures, C.I., Selph, K.E., Zhou, M., Hisock, W.T., 2013. Iron fluxes from the shelf regions near the South Shetland Islands in the Drake Passage during the austral-winter 2006. Deep-Sea Res. II 90, 89–101.

Hawkes, J.A., Connelly, D.P., Gledhill, M., Achterberg, E.P., 2013. The stabilization and transportation of dissolved iron from high temperature hydrothermal vent systems. Earth Planet. Sci. Lett. 375, 280–290.

Holland, D.M., Jacobs, S.S., Jenkins, A., 2003. Modelling the ocean circulation beneath the Ross Ice Shelf. Antarct. Sci. 15, 13–23.

Hosegood, P., van Haren, H., Veth, C., 2005. Mixing within the interior of the Faeroe-Shetland Channel. J. Mar. Res. 63, 529–561.

Jacobs, S.S., Giulivi, C., 1998. Interannual ocean and sea ice variability in the Ross Sea. Antarct. Res. Ser. 75, 135–150.

Jacobs, S.S., Amos, A.F., Bruchhausen, P.M., 1970. Ross Sea oceanography and Antarctic Bottom Water formation. Deep-Sea Res. 17, 935–962.

Jacobs, S.S., Giulivi, C.F., Mele, P.A., 2002. Freshening of the Ross Sea during the late 20th century. Science 297, 386–389.

Jacobs, S.S., Jenkins, A., Giulivi, C.F., Dutrieux, P., 2011. Stronger ocean circulation and increase melting under Pine Island Glacier ice shelf. Nat. Geosci. 4 (519–523), 2011. http://dx.doi.org/10.1038/ngeo1188.

Jeandel, C., Rutgers van der Loeff, M., Lam, P.J., Roy-Barman, M., Sherrell, R.M., Kretschmer, S., German, C., Dehairs, F., 2015. What did we learn about ocean particle dynamics in the GEOSECS-JGOFS era? Prog. Oceanogr. 133, 6–16.

Johnson, K.S., Gordon, R.M., Coale, K.H., 1997. What controls dissolved iron concentrations in the world ocean? Mar. Chem. 57, 137–161.

Johnson, K.S., Boyle, E., Bruland, K., Measures, C., Moffett, J., Aquilarislas, A., Barbeau, K., Cai, Y., Chase, Z., Cullen, J., Doi, T., Elrod, V., Fitzwater, S., Gordon, M., King, A., Laan, P., Laglera-Baquer, L., Landing, W., Lohan, M., Mendez, J., Milne, A., Obata, H., Ossiander, L., Plant, J., Sarthou, G., Sedwick, P., Smith, G.J., Sohst, B., Tanner, S., Van Den Berg, S., Wu, J., 2007. Developing standards for dissolved iron in seawater. Eos. Trans. 88, 131.

Jones, E.M., Bakker, D.C.E., Venables, H.J., Hardman-Mountford, N., 2015. Seasonal cycle of CO₂ from the sea ice edge to island blooms in the Scotia Sea, Southern Ocean. Mar. Chem. 177, 490–500 (in this issue).

Klunder, M.B., Laan, P., Middag, R., De Baar, H.J.W., van Ooijen, J.C., 2011. Dissolved Fe in the Southern Ocean (Atlantic sector). Deep-Sea Res. II 58, 2678–2694.

Klunder, M.B., Laan, P., Middag, R., De Baar, H.J.W., Bakker, K., 2012. Dissolved iron in the Arctic Ocean: important role of hydrothermal sources, shelf input and scavenging removal. J. Geophys. Res. 117, C04014. http://dx.doi.org/10.1029/2011JC007135.

Lannuzel, D., Schoemann, V., de Jong, J., Pasquer, B., van der Merwe, P., Masson, F., Tison, J.-L., Bowie, A., 2010. Distribution of dissolved iron in Antarctic sea ice: spatial, seasonal, and inter-annual variability. J. Geophys. Res. 115, G03022. http://dx.doi.org/10.1029/2009JG001031.

Lannuzel, D., van der Merwe, P.C., Townsend, A.T., Bowie, A.R., 2014. Size fractionation of iron, manganese and aluminium in Antarctic fast ice reveals a lithogenic origin and low iron solubility. Mar. Chem. 161, 47–56.

Liu, X., Millero, F.J., 2002. The solubility of iron in seawater. Mar. Chem. 77, 43–54.

Löscher, B.M., De Baar, H.J.W., De Jong, J.T.M., Veth, C., Dehairs, F., 1997. The distribution of Fe in the Antarctic Circumpolar Current. Deep-Sea Res. II 44, 143–187.

Marsay, C.M., Sedwick, P.N., Dinniman, M.S., Barrett, P.M., Mack, S.L., McGillicuddy, D.J., 2014. Estimating the benthic efflux of dissolved iron on the Ross Sea continental shelf. Geophys. Res. Lett. 41, 7576–7583. http://dx.doi.org/10.1002/2014GL061684.

Martin, J.H., Fitzwater, S.E., Gordon, R.M., 1990. Iron deficiency limits phytoplankton growth in Antarctic waters. Glob. Biogeochem. Cycles 4, 5–12.

Martin, J.H., Coale, K.H., Johnson, K.S., Fitzwater, S.E., Gordon, R.M., Tanner, S.J., Hunter, C.N., Elrod, V.A., Nowicki, J.L., Coley, T.L., Barber, R.T., Lindley, S., Watson, A.J., van Scoy, K., Law, C.S., Liddicoat, M.I., Ling, R., Station, T., Stockel, J., Collins, C., Anderson, A., Bidigare, R., Ondrusek, M., Latasa, M., Millero, F.J., Lee, K., Yao, W., Zhang, J.Z., Friederich, G., Sakamoto, C., Chavez, F., Buck, K., Kolber, Z., Green, R., Falkowski, P., Chisholm, S.W., Hoge, F., Swift, R., Yangel, J., Turner, S., Nightingale, P., Hatton, A., Liss, P., Tindale, N.W., 1994. Testing the iron hypothesis in ecosystems of the equatorial Pacific Ocean. Nature 371, 123–129.

McDougall, T.J., Feistel, R., Millero, F.J., Jackett, D.R., Wright, D.G., King, B.A., Marion, G.M., Chen, C.T.A., Spitzer, P., 2009. Calculation of the thermodynamic properties of seawater, Global ship-based repeat hydrography manual. IOCCP Report 14. ICPO Publication Series 134. U.N.E.S.C.O., Paris, France, p. 131.

Middag, R., de Baar, H.J.W., Laan, P., Klunder, M.B., 2011. Fluvial and hydrothermal input of manganese into the Arctic Ocean. Geochim. Cosmochim. Acta 75, 2393–2408.

Millero, F.J., 1998. Solubility of Fe(III) in seawater. Earth Planet. Sci. Lett. 154, 323–330.

Mitchell, B.G., Brody, E.A., Holm-Hansen, O., McClain, C., Bishop, J., 1991. Light limitation of phytoplankton biomass and macronutrient utilization in the Southern Ocean. Limnol. Oceanogr. 36, 1662–1677.

Okubo, A., 1971. Oceanic diffusion diagrams. Deep-Sea Res. 18, 789–802.

Orsi, A.H., Wiederwohl, C.L., 2009. A recount of Ross Sea waters. Deep-Sea Res. II 56, 778–795.

Planquette, H., Statham, P.J., Fones, G.R., Charette, M.A., Moore, C.M., Salter, I., Nédélec, F.H., Taylor, S.L., French, M., Baker, A.R., Mahowald, N., Jickells, T.D., 2007. Dissolved iron in the vicinity of the Crozet Islands, Southern Ocean. Deep-Sea Res. II 54, 1999–2019.

Raiswell, R., Tranter, M., Benning, L.G., Siegert, M., Death, R., Huybrechts, P., Payne, T., 2006. Contributions from glacially derived sediment to the global iron (oxyhydr)oxide cycle: implications for iron delivery to the oceans. Geochim. Cosmochim. Acta 70, 2765–2780.

Raiswell, R., Benning, L.G., Tranter, M., Tulaczyk, S., 2008. Bioavailable iron in the Southern Ocean: the significance of the iceberg conveyor belt. Geochem. Trans. 9, 7. http://dx.doi.org/10.1186/1467-4866-9-7.

Reddy, T.E., Arrigo, K.R., 2006. Constraints on the extent of the Ross Sea phytoplankton bloom. J. Geophys. Res. 111 (C7), C07005. http://dx.doi.org/10.1029/2005JC003339.

Rignot, E., Jacobs, S., Mouginot, J., Scheuchl, B., 2013. Ice-shelf melting around Antarctica. Science 341, 266–270.

Sarmiento, J.L., Slater, R., Barber, R., Bopp, L., Doney, S.C., Hirst, A.C., Kleypas, J., Matear, R., Mikolajewicz, U., Monfray, P., Soldatov, V., Spall, S.A., Stouffer, R., 2004. Response of ocean ecosystems to climate warming. Glob. Biogeochem. Cycles 18, GB3003. http://dx.doi.org/10.1029/2003GB002134.

Sedwick, P.N., DiTullio, G.R., 1997. Regulation of algal blooms in Antarctic shelf waters by the release of iron from melting sea ice. Geophys. Res. Lett. 24, 2515–2518.

Sedwick, P.N., DiTullio, G.R., Mackey, D.J., 2000. Iron and manganese in the Ross Sea, Antarctica: seasonal iron limitation in Antarctic shelf waters. J. Geophys. Res. 105, 11321–11336.

Sedwick, P.N., Bowie, A.R., Trull, T.W., 2008. Dissolved iron in the Australian sector of the Southern Ocean (CLIVAR SR3 section): meridional and seasonal trends. Deep-Sea Res. I 55, 911–925.

Sedwick, P.N., Marsay, C.M., Sohst, B.M., Aguilar-Islas, A.M., Lohan, M.C., Long, M.C., Arrigo, K.R., Dunbar, R.B., Saito, M.A., Smith, W.O., Di Tullio, G.R., 2011. Early season depletion of dissolved iron in the Ross Sea polynya: implications for iron dynamics on the Antarctic continental shelf. J. Geophys. Res. 116, C12019.

Sherrell, R.M., Lagerström, M., Forsch, K., Stammerjohn, S.E., Yager, P.L., (2015). Dynamics of dissolved iron and other bioactive trace metals (Mn, Ni, Cu, Zn) in the Amundsen Sea Polynya, Antarctica. Elem Sci Anth (submitted).

Smith, W.O. (Ed.), 2007. Polynyas: windows to the world. Elsevier Oceanography Series vol. 74. Elsevier, Amsterdam.

Smith Jr., W.O., Dinniman, M.S., Klinck, J.M., Hoffman, E., 2003. Biogeochemical climatologies in the Ross Sea, Antarctica: seasonal patterns of nutrients and biomass. Deep-Sea Res. II 50, 3083–3101.

Smith, W.O., Shields, A.R., Peloquin, J.A., Catalano, G., Tozzi, S., Dinniman, M.S., Asper, V.A., 2006. Interannual variations in nutrients, net community production, and biogeochemical cycles in the Ross Sea. Deep-Sea Res. II 53, 815–833.

Smith Jr., W.O., Sedwick, P.N., Arrigo, K.R., Ainley, D.G., Orsi, A.H., 2012. The Ross Sea in a sea of change. Oceanography 25, 90–103. http://dx.doi.org/10.5670/oceanog.2012.80.

Stansfield, K., Garrett, C., Dewey, R., 2001. The probability distribution of the Thorpe displacement within overturns in Juan de Fuca Strait. J. Phys. Oceanogr. 31, 3421–3434.

Strzepek, R.F., Maldonado, M.T., Hunter, K.A., Frew, R.D., Boyd, P.W., 2011. Adaptive strategies by Southern Ocean phytoplankton to lessen iron limitation: uptake of organically complexed iron and reduced cellular iron requirements. Limnol. Oceanogr. 56, 1983–2002.

Tagliabue, A., Bopp, L., Dutay, J.-C., Bowie, A.R., Chever, F., Jean-Baptiste, P., Bucciarelli, E., Lannuzel, D., Remenyi, T., Sarthou, G., Aumont, O., Gehlen, M., Jeandel, C., 2010. Hydrothermal contribution to the oceanic dissolved iron inventory. Nat. Geosci. 14, 1–5. http://dx.doi.org/10.1038/NGEO818.

Thompson, P.A., Guo, M., Harrison, P.J., 1992. Effects of variation in the temperature. I. On the biochemical composition of eight species of marine phytoplankton. J. Phycol. 28, 481–488.

Thorpe, S.A., 1977. Turbulence and mixing in a Scottish loch. Philos. Trans. R. Soc. Lond. A 286, 125–181.

Thuróczy, C.-E., Gerringa, L., Klunder, M., Laan, P., De Baar, H., 2011. Observation of consistent trends in the organic complexation of dissolved iron in the Atlantic sector of the Southern Ocean. Deep-Sea Res. II 58, 2695–2706.

Thuróczy, C.-E., Alderkamp, A.-C., Laan, P., Gerringa, L.J.A., De Baar, H.J.W., Arrigo, K.R., 2012. Key role of organic complexation of iron in sustaining phytoplankton blooms in the Pine Island and Amundsen Polynyas (Southern Ocean). Deep-Sea Res. II 71–76, 49–60.

Timmermans, K.R., Gerringa, L.J.A., de Baar, H.J.W., van der Wagt, B., Veldhuis, M.J.W., de Jong, J.T.M., Croot, P.L., Boye, M., 2001. Growth rates of large and small Southern Ocean diatoms in relation to availability of iron in natural seawater. Limnol. Oceanogr. 46, 260–266. http://dx.doi.org/10.4319/lo.2001.46.2.0260.

Timmermans, K.R., van der Wagt, B., de Baar, H.J.W., 2004. Growth rates, half-saturation constants, and silicate, nitrate, and phosphate depletion in relation to iron availability of four large, open-ocean diatoms from the Southern Ocean. Limnol. Oceanogr. 49, 2141–2151. http://dx.doi.org/10.4319/lo.2004.49.6.2141.

Tomczak, M., Godfrey, J.S., 2001. Regional Oceanography: An Introduction. Elsevier, Oxford.

Twining, B.S., Baines, S.B., Fischer, N.S., 2004. Element stoichiometries of individual plankton cells collected during the Southern Ocean Iron Experiment (SOFeX). Limnol. Oceanogr. 49, 2115–2212.

van der Merwe, P., Lannuzel, D., Bowie, A.R., Meiners, K.M., 2011. High temporal resolution observations of spring fast-ice melt and seawater iron enrichment in East Antarctica. J. Geophys. Res. 116, G03017. http://dx.doi.org/10.1029/2010JG001628.

van Haren, H., Gostiaux, L., 2014. Characterizing turbulent overturns in CTD-data. Dyn. Atmos. Oceans 66, 58–76.

Wadham, J.L., Death, R., Monteiro, F.M., Tranter, M., Ridgwell, A., Raiswell, R., Tulaczyk, S., 2013. The potential role of the Antarctic Ice Sheet in global biogeochemical cycles. Earth Environ. Sci. Trans. R. Soc. Edinb. 104, 1–13.